

SWOT Nadir GDR 1-day CalVal Phase Report

2023-01-16 09:16:50 to 2023-07-10 08:21:00

Processing Baseline S v2.01

Reference: SALP-RP-MA-EA-23718-CLS

Nomenclature: SWOT Nadir GDR: 1-day CalVal Phase Report

Issue: 01/04

Date: November 17, 2025

Project:	SALP MISSION PERFORMANCE SERVICE FOR SWOT NADIR MISSION				
Title:	SWOT Nadir GDR: 1-day CalVal Phase Report				
Author(s):	N. Kientz, ALTEN for CLS				
	A. Deniau, CLS				
	T. Pirotte, CLS				
	H. Roinard, CLS				
Approved by:	F. Bignalet-Cazalet, CNES	Application authorized by:	N. Picot, CNES		



Change Log

Version	Date	Changes
1.0	April 25, 2025	Creation
1.1	September 26, 2025	Add of the section: Comparison to DUACS DT-24 & Some improvements
1.2	October 21, 2025	Add information in section 4 "Monitoring of altimeter parameter" & Some improvements
1.3	November 13, 2025	Add latitudinal graph for Xover & Improvements with references
1.4	November 17, 2025	Add Xover with data selection (far from coast)



Acronyms

CNES Centre National d'Etudes Spatiales

CNG Consigne Numerique de Gain (= Automatic Gain Control)

DAC Dynamical Atmospheric Correction

DTC Dry Tropospheric Correction

DV Default Value

MSS Mean Sea Surface

POD Precise Orbit Determination

POS-3C POSEIDON-3C

Sigma0 Backscatter coefficient

SSH Sea Surface Height

SSHA Sea Surface Height Anomaly

SLA Sea Level Anomaly

SSR Solid State Recorder

SSB Sea State Bias

SWH Significant Wave Height

WTC Wet Tropospheric Correction



Table of Content

1	Introduction	10
2	Processing Status 2.1 Data used	11 14 15
3	Data coverage and edited measurements 3.1 Missing measurements 3.2 Edited measurements 3.2.1 Editing 3.2.2 Flagging quality criterion: Ice flag 3.2.3 Editing on threshold criteria 3.2.3.1 Overview 3.2.3.2 Threshold criteria: 20-Hz range measurements number and standard deviation 3.2.3.3 Threshold criteria: Significant wave height (SWH) 3.2.3.4 Threshold criteria: Waveform-derived square off nadir angle 3.2.3.5 Threshold criteria: Sigma0 3.2.3.6 Threshold criteria: Altimeter wind speed 3.2.3.7 Threshold criteria: Sea State Bias 3.2.3.8 Threshold criteria: Ionospheric correction 3.2.3.9 Threshold criteria: Radiometer Wet Troposphere Correction 3.2.3.10 Threshold criteria: Ocean tide 3.2.3.11 Threshold criteria: Sea Surface height 3.2.3.12 Threshold criteria: Sea Surface Height Anomaly	18 19 19 19 21 24 26 27 31 33 35 37 39
4	Monitoring of altimeter parameters 4.1 20 Hz measurements 4.2 Off-nadir angle from waveform 4.3 Significant wave height 4.4 Backscatter coefficient 4.5 Wind speed 4.6 Sea State Bias Correction 4.7 Ionospheric correction	44 45 46 47 49
5	Validation and Monitoring of Radiometer Parameters 5.1 Geophysical products monitoring 5.2 Comparison with Sentinel-6A 5.3 Intercalibration monitoring 5.4 Degraded interpolation	54 55
6	Multimission comparison6.1 Assessment from crossover analysis6.2 Comparison to DUACS DT-246.3 Mean and Standard deviation of SSHA	61
7	Conclusions	66
8	Annexes	67
9	References	68



List of Figures

1	Different POS-3C CNG calibration locations	13
2	SWOT Nadir Acquisition and Tracking modes per pass	15
3	SWOT Nadir GDR data availability wrt theoretical coverage	17
4	SWOT Nadir GDR data availability wrt theoretical coverage over ocean	17
5	Map of SWOT Nadir GDR data validity wrt available coverage over ocean	18
6	SWOT Nadir GDR data validity wrt available coverage over ocean (colored lines correspond to maneuvers in Table 2)	18
7	Ice flag editing: monitoring and spatial distribution	19
8	Data editing by thresholds over ocean, average by cycle	19
9	Data editing by thresholds over ocean, map	20
10	Cyclic monitoring of rejected measurements rate due to range number of 20Hz elementary measurements criterion	21
11	Maps of rejected/discarded measurements due to range number of 20Hz elementary measurements criterion	22
12	Cyclic monitoring of rejected measurements rate due to range std of 20Hz elementary measurements criterion	23
13	Maps of rejected/discarded measurements due to range std of 20Hz elementary measurements criterion	23
14	Cyclic monitoring of rejected measurements rate due to SWH criterion	24
15	Maps of rejected/discarded measurements due to SWH criterion	25
16	Cyclic monitoring of rejected measurements rate due to mispointing criterion	26
17	Maps of rejected/discarded measurements due to mispointing criterion	26
18	Cyclic monitoring of rejected measurements rate due to sigma0 number of 20Hz elementary measurements criterion	27
19	Maps of rejected/discarded measurements due to Sigma0 number of 20Hz elementary measurements criterion	28
20	Cyclic monitoring of rejected measurements rate due to sigma0 std of 20Hz elementary measurements criterion	29
21	Maps of rejected/discarded measurements due to Sigma0 std of 20Hz elementary measurements criterion	29
22	Cyclic monitoring of rejected measurements rate due to sigma0 criterion	30
23	Maps of rejected/discarded measurements due to Sigma0 criterion	30
24	Cyclic monitoring of rejected measurements rate due to Wind Speed criterion	31
25	Maps of rejected/discarded measurements due to Wind Speed criterion	32



26	Cyclic monitoring of rejected measurements rate due to Sea State Bias criterion	33
27	Maps of rejected/discarded measurements due to Sea State Bias criterion	34
28	Cyclic monitoring of rejected measurements rate due to ionospheric correction criterion	35
29	Maps of rejected/discarded measurements due to Ionospheric correction criterion	36
30	Cyclic monitoring of rejected measurements rate due to Wet Troposphere Correction criterion .	37
31	Maps of rejected/discarded measurements due to WTC criterion	38
32	Cyclic monitoring of rejected measurements rate due to ocean tide criterion	39
33	Cyclic monitoring of rejected measurements rate due to Sea Surface Height criterion	39
34	Maps of rejected/discarded measurements due to Sea Surface Height criterion	40
35	Cyclic monitoring of rejected measurements rate due to Sea Surface Height Anomaly criterion	41
36	Maps of rejected/discarded measurements due to Sea Surface Height Anomaly criterion	42
37	Cyclic monitoring of elementary 20 Hz range and sigma0 measurements	43
38	Maps of the 20Hz range measurements, number (left) and std (right).	44
39	Cyclic monitoring of the square off-nadir angle mean (left) and standard deviation (right)	44
40	Monitoring of significant wave height (top) and difference to ERA5 swh (bottom). Mean (left) and standard deviation (right)	45
41	Maps of the SWH MLE4 difference with ERA5 model, mean (left) and standard deviation (right).	45
42	Histogram: SWH ERA5 vs MLE4	46
43	Cyclic monitoring of sigma0 measurements, mean (left) and standard deviation (right)	46
44	Monitoring of wind speed (top) and difference to ERA5 wind speed (bottom). Mean (left) and standard deviation (right)	47
45	Maps of the wind speed MLE4 difference with ERA5 model, mean (left) and standard deviation (right)	48
46	Histogram: Wind speed ERA5 vs MLE4	48
47	Monitoring of sea state bias	49
48	Monitoring of ionospheric correction (top) and difference to GIM iono. corr. (bottom). Mean (left) and standard deviation (right)	50
49	Along track monitoring of ionospheric correction for C501 P13	51
50	Temporal monitoring of ionospheric correction measurements lost by filtering	51
51	Monitoring of lost ionospheric correction points through filtering	52
52	Daily monitoring of the mean of the Wet Tropospheric Correction for the AMR S1 (blue), AMR S2 (orange) and Nadir (green) for the entire calval phase	53



53	Daily monitoring of the mean of the Wet Tropospheric Correction for the AMR S1 (blue), AMR S2 (orange) and Nadir (green) for the entire calval phase	54
54	Daily monitoring of the mean of the Wet Tropospheric Correction for the AMR S1 (blue), AMR S2 (orange) and Nadir (green) for the entire calval phase	54
55	Comparison of MWR-derived wet tropospheric correction for SWOT Nadir (black solid line) and Sentinel-6A-MF (pink solid line) with those from ECMWF model. (a) Daily mean of Wet Tropospheric Corrections difference (b) Daily standard deviation of Wet Tropospheric Corrections difference, also for AMR Side 1 (green solid line)	55
56	Daily monitoring of the mean S1/S2 gradients of brightness temperatures, for the 18.7 Ghz channel (blue), the 23.4 GHz channel (green) and the 34 GHz channel (red)	56
57	Daily monitoring of the wet tropospheric correction gradient between AMR Side 1 and AMR Side 2 (purple), AMR Side 1 and Nadir (cyan)	56
58	Left: Example of area where the Nadir interpolation quality flag is raised as degraded (orange) due to the rejection of radiometer measurements (red). Right: Evolution of the wet tropospheric correction depending on the latitude in the same example as the left figure, for both AMR sides (Blue and Orange, only valid measurements shown) and Nadir (plain green: valid WTC, dotted green: degraded wtc)	57
59	Proportion of degraded and missing Nadir interpolated wet tropospheric correction by geographical box of 1 degree	57
60	Count daily monitoring of SSH difference at crossovers between SWOT Nadir and Sentinel-6 MF LR	60
61	SSH difference at crossovers between SWOT Nadir and Sentinel-6 MF LR	60
62	Daily monitoring of the mean bias between DUACS and SWOT Nadir SLA	61
63	Daily monitoring of the latitudinal mean bias between DUACS and SWOT Nadir SLA	62
64	Monthly maps of the differences between DUACS and SWOT Nadir	63
65	Daily monitoring of along-track mean SLA	65
66	Daily monitoring of along-track std SLA	65



List of Tables

1	Types of maneuvers and expected impacts	11
	List of maneuvers on calval phase SWOT Nadir mission	
3	POS-3C Calibration (CNG) on calval phase SWOT Nadir mission.	13
4	SWOT Nadir Acquisition Mode	14
	Main SWOT mission events with major impact on data availability	
6	Table of parameters used for editing	20
7	Proportion of each Nadir interpolation quality flag state in open ocean	
8	Entirely missing passes	67



1 Introduction

SWOT (Surface Water Ocean Topography) is a joint project including NASA, Centre National d'Etudes Spatiales (CNES), the Canadian Space Agency and the UK Space Agency. The SWOT satellite carries onboard a wide-swath altimeter-interferometer in Ka-Band (KaRIn), a classical nadir-looking altimeter, as well as the usual complement on altimetry satellites: precise location systems and radiometer.

The SWOT Nadir Quality Assessment report are generated under SALP contract supported by CNES at the CLS Environment & Climate Business Unit. Cyclic assessment reports are made and are available on Aviso website [1].

A detailed description of the mission is available on AVISO website [2]. Products description can be found in the SWOT Level-2 Nadir Altimeter products User Guide [3] and dataset standards for GDR-F are described in the Jason-3 user handbook [4]. The changes between GDR-F and GDR-S2 for SWOT Nadir are specified in the release note [5].

The present document assesses SWOT Nadir data quality and mission performance **over ocean**. After an executive summary in the following pages, dedicated sections of this report deal with:

- · description of data processing,
- · data coverage / availability,
- · monitoring of rejected spurious data,
- analysis of relevant parameters derived from instrumental measurements and geophysical corrections,
- multimission comparissions for sea surface height crossovers and sea level anomalies.

This document focuses only on the 1-day "calval" repetitive orbit phase (that can be referred as calval phase, calval 1-day phase, 1-day phase, fast orbit phase). Another type of document, called "Annual report", is dedicated to the 21-day Science Phase. The 2024 Annual Report is already available here [6]. Thus, the period covered by this issue extends from cycle 402 pass 1 (2023-01-16 09:16:50) to cycle 578 pass 3 (2023-07-10 08:21:00).

Note that data were initially distributed using GDR-F standard, then reprocessed in GDR-S2 standard. This document assess the reprocessed GDR-S2 version.



2 Processing Status

2.1 Data used

Metrics provided in this document are based on SWOT Nadir dataset of the calibration-validation phase (calval), operating on a 1-day repeat orbit from cycle 402 to 578, spanning from 2023-01-16 09:16:50 to 2023-07-10 08:21:00. On this orbit, each cycle as a duration of approximately 23 hours and 51 minutes. GDR data used are 1Hz data unless specified otherwise.

2.2 List of events

Table 1 shows the different maneuver types and their expected impact on data. Some maneuvers (colored ones in Table 1) have an impact over data validity. In the temporal monitoring figures, those maneuvers are highlighted by colored vertical lines. Moreover, OCM_SLOT and NON_REF_ALT impact data availability. As a consequence the ratio of edited data over available ocean points is also affected.

Maneuver type	Expected impact	
CALGYR_SLOT (gyroscope calibration)	Data rejected on editing criteria at DV on retracking and radiometer output variables	
CNG Calibration (POSEIDON-3C in calibration mode)	Data unavailable	
OCM_SLOT (burst for station keeping maneuver)	Data partially rejected or data unavailable	
NON_REF_ALT (avoidance maneuver)	Data rejected or unavailable at the beginning and end of a maneuver in the burst period	
SADM_CRUISE_SLOT (change of solar panel position)	No rejected data, no loss of coverage	
YAWFLIP_SLOT (satellite flip-over)	Data rejected on editing criteria at Default Value (DV) on retracking and radiometer output variables	

Table 1: Types of maneuvers and expected impacts

Table 2 bellow lists all the events that occured during the calval phase.

Note that the sequence of an OCM_SLOT maneuver, followed by a NON_REF_ALT maneuver and again an OCM_SLOT maneuver corresponds to the complete sequence of an avoidance maneuver, the sequence is writting in blue in Table 2.

Event	Cycle	Pass	Start date	End date
SADM CRUISE SLOT	406	6	2023-01-20 12:59:14	2023-01-20 13:03:44
OCM SLOT	408	15-16	2023-01-22 20:50:16	2023-01-22 21:27:32
NON REF ALT	408	16-19	2023-01-22 21:27:32	2023-01-23 00:14:37
OCM SLOT	408	19-20	2023-01-23 00:14:37	2023-01-23 00:51:54
CALGYR SLOT	410	2	2023-01-24 09:00:23	2023-01-24 09:30:23
CALGYR SLOT	410-411	20-2	2023-01-25 00:19:43	2023-01-25 09:19:09
OCM SLOT	412	25-26	2023-01-27 04:40:20	2023-01-27 05:17:24
OCM SLOT	416	21-22	2023-01-31 00:33:06	2023-01-31 01:10:21
OCM SLOT	416-417	28-1	2023-01-31 06:30:44	2023-01-31 07:07:58
SADM CRUISE SLOT	418	6	2023-02-01 11:24:18	2023-02-01 11:28:48
SADM CRUISE SLOT	418	10	2023-02-01 14:54:02	2023-02-01 14:58:32
OCM SLOT	424	22-23	2023-02-08 00:17:45	2023-02-08 00:54:46
NON REF ALT	424-425	23-2	2023-02-08 00:54:46	2023-02-08 07:06:30
OCM SLOT	425	2-3	2023-02-08 07:06:30	2023-02-08 07:43:31
OCM SLOT	426	22-23	2023-02-09 23:57:45	2023-02-10 00:34:46



Event	Cycle	Pass	Start date	End date
NON REF ALT	426-427	23-2	2023-02-10 00:34:46	2023-02-10 06:46:30
OCM SLOT	427	2-3	2023-02-10 06:46:30	2023-02-10 07:23:31
OCM SLOT	430	24-25	2023-02-14 01:07:46	2023-02-14 01:44:48
NON REF ALT	430-431	25-2	2023-02-14 01:44:48	2023-02-14 06:14:20
OCM SLOT	431	2-3	2023-02-14 06:14:20	2023-02-14 06:51:22
OCM SLOT	434	2-3	2023-02-17 05:40:47	2023-02-17 06:17:53
OCM SLOT	455	7-8	2023-03-10 06:38:29	2023-03-10 07:15:36
SADM CRUISE SLOT	462	5	2023-03-17 03:26:43	2023-03-17 03:31:13
OCM SLOT	469	9-10	2023-03-24 05:54:57	2023-03-24 06:32:01
SADM CRUISE SLOT	470	13	2023-03-25 08:59:55	2023-03-25 09:04:25
YAWFLIP SLOT	472	27	2023-03-27 20:37:02	2023-03-27 20:59:37
OCM SLOT	475	12-13	2023-03-30 07:50:14	2023-03-30 08:27:27
NON REF ALT	475	13-24	2023-03-30 08:27:27	2023-03-30 18:03:20
OCM SLOT	475	24-25	2023-03-30 18:03:20	2023-03-30 18:40:33
SADM CRUISE SLOT	476	1	2023-03-30 21:50:46	2023-03-30 21:55:16
OCM SLOT	481	27-28	2023-04-05 19:20:18	2023-04-05 19:57:22
SADM CRUISE SLOT	483	27	2023-04-07 18:54:40	2023-04-07 18:59:10
CALGYR SLOT	489	18	2023-04-13 10:15:30	2023-04-13 10:45:30
OCM SLOT	498	2-3	2023-04-21 19:59:08	2023-04-21 20:36:11
OCM SLOT	512	4-5	2023-05-05 19:22:53	2023-05-05 19:59:55
OCM SLOT	520	7-8	2023-05-13 20:31:41	2023-05-13 21:08:44
NON REF ALT	520	8-11	2023-05-13 21:08:44	2023-05-13 23:56:04
OCM SLOT	520	11-12	2023-05-13 23:56:04	2023-05-14 00:33:06
OCM SLOT	524	8-9	2023-05-17 20:55:30	2023-05-17 21:32:34
OCM SLOT	539	18-19	2023-06-02 02:45:06	2023-06-02 03:22:09
SADM CRUISE SLOT	541	10	2023-06-03 19:28:31	2023-06-03 19:33:01
SADM CRUISE SLOT	550	4	2023-06-12 12:57:42	2023-06-12 13:02:12
YAWFLIP SLOT	552	26	2023-06-15 07:23:52	2023-06-15 07:45:57
OCM SLOT	554	12-13	2023-06-16 19:24:42	2023-06-16 20:01:46
SADM CRUISE SLOT	555	20	2023-06-18 01:49:13	2023-06-18 01:53:43
SADM CRUISE SLOT	564	26	2023-06-27 05:34:31	2023-06-27 05:39:01
OCM SLOT	568	14	2023-06-30 18:37:01	2023-06-30 19:14:04
CALGYR SLOT	571-572	28-11	2023-07-04 06:16:11	2023-07-04 15:15:37
Move to science orbit	578		2023-07-10 08:10:12	

Table 2: List of maneuvers on calval phase SWOT Nadir mission.



Calibration	Cycle	Pass	Start date	End date
Cal CNG	402	8-9	2023-01-16 16:00:00	2023-01-16 16:33:03
Cal CNG	414	2	2023-01-28 08:23:30	2023-01-28 08:56:33
Cal CNG	414	13	2023-01-28 17:46:30	2023-01-28 18:19:33
Cal CNG	421	5-6	2023-02-04 10:16:00	2023-02-04 10:49:03
Cal CNG	421	13-14	2023-02-04 16:53:00	2023-02-04 17:26:03
Cal CNG	456	28	2023-03-12 00:00:00	2023-03-12 00:33:03
Cal CNG	457	26	2023-03-12 22:10:00	2023-03-12 22:43:03
Cal CNG	554	1	2023-06-16 09:50:00	2023-06-16 10:23:03

Table 3: POS-3C Calibration (CNG) on calval phase SWOT Nadir mission.

The corresponding locations of POSEIDON-3C (POS-3C) Consigne Numerique de Gain (= Automatic Gain Control) (CNG) calibrations can be found in figure 1.

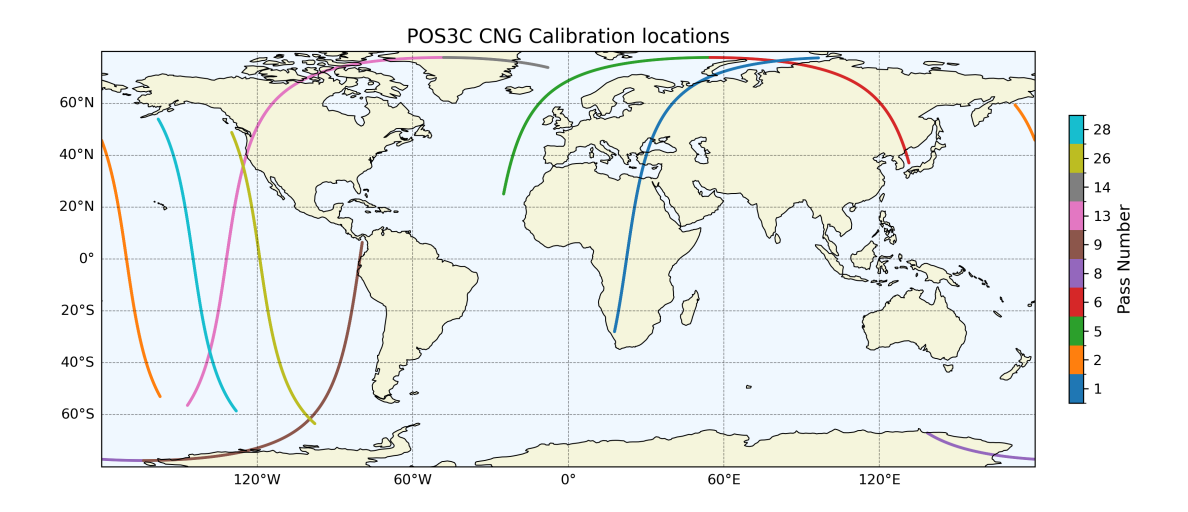


Figure 1: Different POS-3C CNG calibration locations



2.3 Tracking and acquisition mode

SWOT Nadir is able to track data with several onboard tracker modes: POSEIDON-3C instrument implements five tracking modes:

- The autonomous acquisition and tracking mode (M1)
- The DIODE acquisition and autonomous tracking mode (M2)
- The DIODE & DEM mode (M3)
- The DIODE + DEM Tracking with Auto transition (M4)
- The DIODE + DEM Tracking with Auto transition and direct acquisition from Open Loop to Closed loop (M4bis)

Certain automatic transitions can be authorized by the user, as is the case in M4 to M4bis modes.

The different tracking modes are described in the article of Guérin *et al.* [7]. The status of tracking and acquisition modes are detailed in Table 4.

The acquisition mode as shown corresponds to the netcdf field <code>alt_state_acq_mode_flag</code> which is the 20Hz altimeter state flag for operational acquisition mode. This flag can take 3 values: "8" for autonomous acquisition / tracking, "9" for autonomous DIODE acquisition / tracking and "10" for DIODE + Digital Elevation Model tracking.

The tracking mode as shown corresponds to the netcdf field *alt_state_track_trans_flag* which is the 20Hz altimeter state flag for tracking automatic transition. This flag can take 2 values: "0" for authorized and "1" for inhibited.

Those modes variations are represented in Figure 2. In this figure flag values are averaged per pass, hence

Date	Cycle-Pass	Acquisition Mode
From 2023-01-16 09:34 to 2023-02-06 01:32	C402 P01 to C422 P23	M1
From 2023-02-06 01:32 to 2023-02-13 03:43	C422 P23 to C429 P27	M2
From 2023-02-13 03:43 to 2023-02-20 04:20	C429 P27 to C437 P01	M3
From 2023-02-20 04:20 to 2023-03-20 00:00	C437 P01 to C465 P01	M4
From 2023-03-20 00:00 to 2023-07-10 08:21	C465 P01 to C578 P03	M4bis

Table 4: SWOT Nadir Acquisition Mode.

it explains the decimal values.



SWOT Nadir acqusition/tracking flag mean per pass

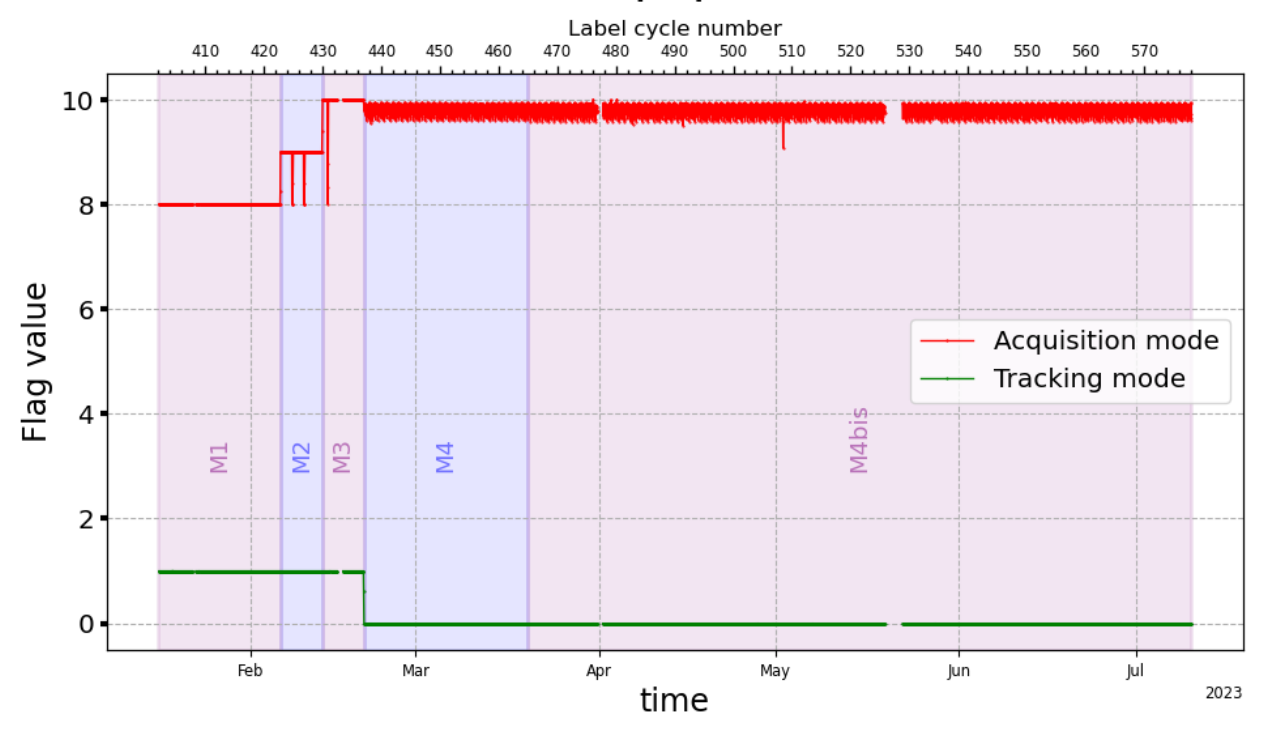


Figure 2: SWOT Nadir Acquisition and Tracking modes per pass

2.4 Processing versions

During the calval phase, the processing baseline version is stable at version S v2.01. The Processing software reference is also stable during the whole period, with the following reference:

- L1_library=V6.2.1
- L2_library=V7.2.3-cal
- Processing_Pilot=5.3.0

2.5 Cautions

Users are advised of the following known limitations in the dataset:

- The adaptive retracker has not yet been calibrated, so the adaptive retracker variables should be used with caution.
- Sea State Bias (SSB) tables are based on Jason-3 training.



3 Data coverage and edited measurements

3.1 Missing measurements

Missing measurements are detected by comparison to SWOT Nadir's theoretical ground track. Various events can affect the data coverage and lead to missing measurements. These events are either planned like special calibrations or unexpected like missing telemetry, reception station problems. The monitoring of the cyclic percentage of available measurements is displayed in Figure 3, and shows the good data coverage, that reaches 94.8% over ocean for the calval fast orbit phase (Figure 4). The table 5 shows the major events impacting data coverage during the calval fast orbit phase of the SWOT mission. Those major events are displayed in purple in the following coverage figures.

Start time to End time	Cycle	Event	
22 Jan 2023	408	Collision avoidance maneuver	
20h50 to 00h33			
14 to 16 Feb 2023	432 to 434	Data gaps due to Solid State Recorder (SSR) EDAC errors	
31 Mar 2023 to 01 Apr 2023	476 to 477	Many gaps on several passes due to high winds at Kiruna + mass memory outage	
19 May 2023 14h16	525 to 528	mass memory outage	
to 22 May 2023 11h			

Table 5: Main SWOT mission events with major impact on data availability



The list of totally missing L2_NALT_GDR products is detailed in section 8 (Annexe): Table of missing products (L2_NALT).

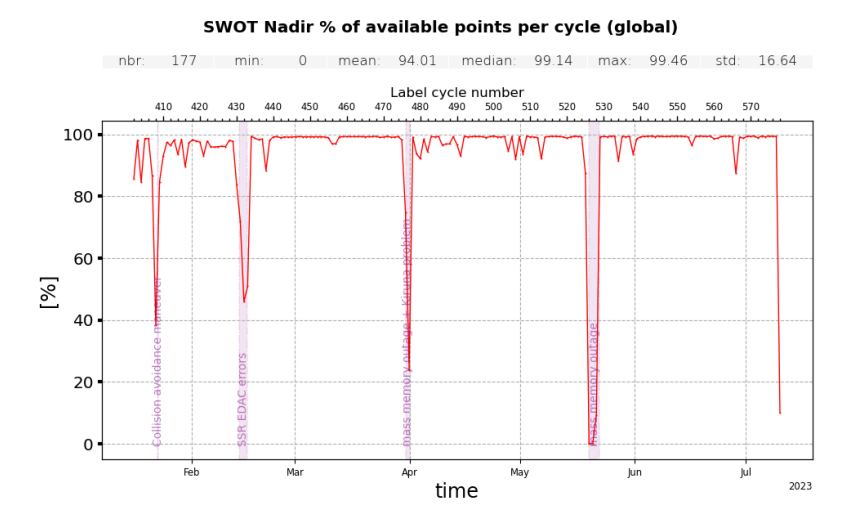


Figure 3: SWOT Nadir GDR data availability wrt theoretical coverage

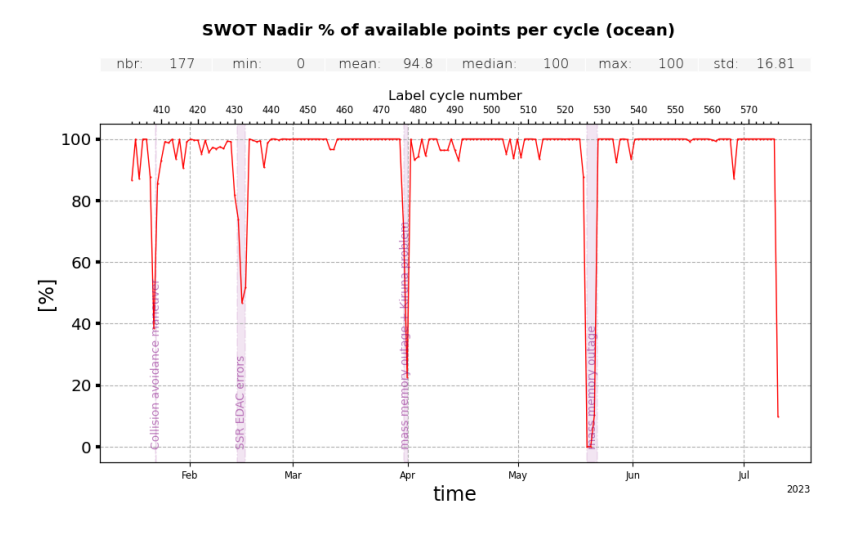


Figure 4: SWOT Nadir GDR data availability wrt theoretical coverage over ocean



3.2 Edited measurements

Editing criteria allow to select only measurements considered as valid over ocean within the available measurements. First a check of the latitude monotony is performed followed by the 3 main steps:

- 1. Measurements over land are removed (*surface_classification_flag* from product different to 0), only measurements over ocean are kept;
- 2. Measurements over ice are removed (ice_flag from product different to 0);
- 3. Threshold criteria are applied on altimeter, radiometer and geophysical parameters as described in the following table 6. This step includes the rejection of measurements at Default Value (DV).

3.2.1 Editing

According to the parameters presented above, the SWOT Nadir data validity rate was 82.33% over ocean. The data validity over this phase is plotted on the map figure 5 and on temporal plot 6.

Percentage of valid ocean points from C402 to C578 30°N 0° 0° 180° 120°W 60°W 0° 60°E 120°E 180° 100 [%]

Figure 5: Map of SWOT Nadir GDR data validity wrt available coverage over ocean

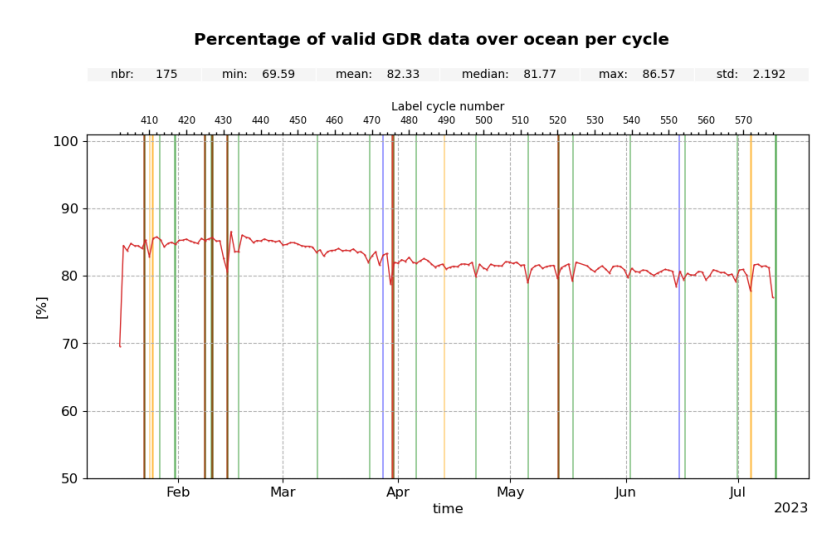


Figure 6: SWOT Nadir GDR data validity wrt available coverage over ocean (colored lines correspond to maneuvers in Table 2)



3.2.2 Flagging quality criterion: Ice flag

The ice flag criterion aims to remove the ice and sea ice data. Figure 7 shows daily percentage of measurements edited by this criterion over ocean. Over the calval phase, in average 14.94% of data were edited by this criterion over ocean.

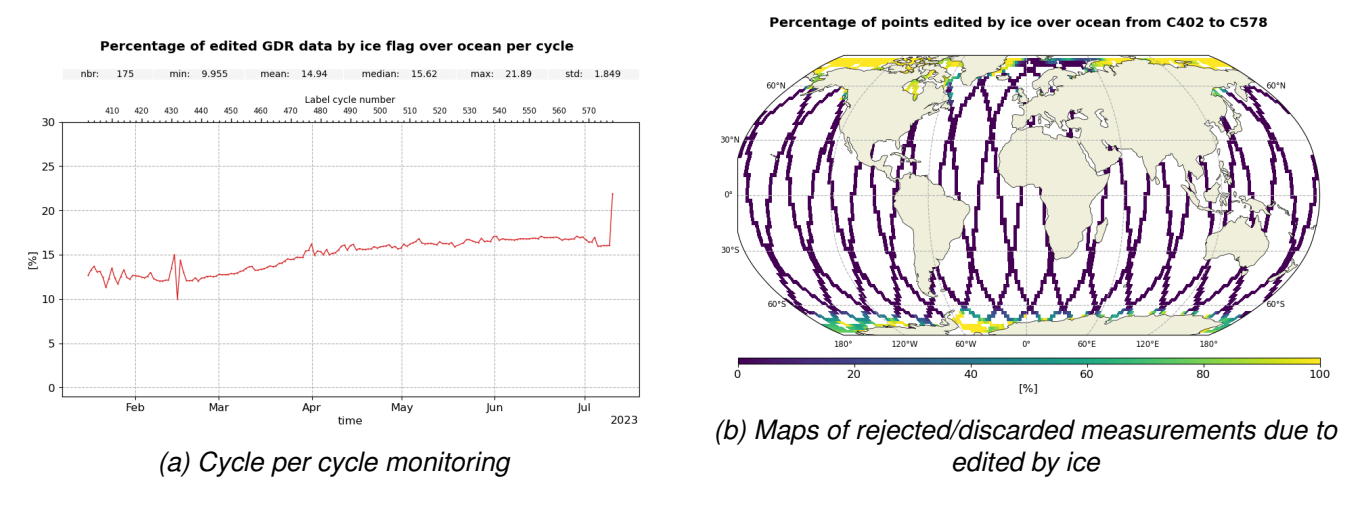


Figure 7: Ice flag editing: monitoring and spatial distribution

3.2.3 Editing on threshold criteria

3.2.3.1 Overview

After quality flag analysis, instrumental parameters have also been analyzed from comparison with thresholds. The average of total edited measurements following threshold criterion is around 2.86% (Figure 8). For each criterion, cyclic percentage of edited measurements is monitored (detailed later). This allows the detection of anomalies in the number of removed data, which could be of instrumental, geophysical or algorithmic origins. Note that all peaks are on maneuver slots (colored lines). Threshold criteria applied on altimeter, radiometer and geophysical parameters are described in the following table 6. The last column represents the mean of rejected data on each criterion over the calval phase.

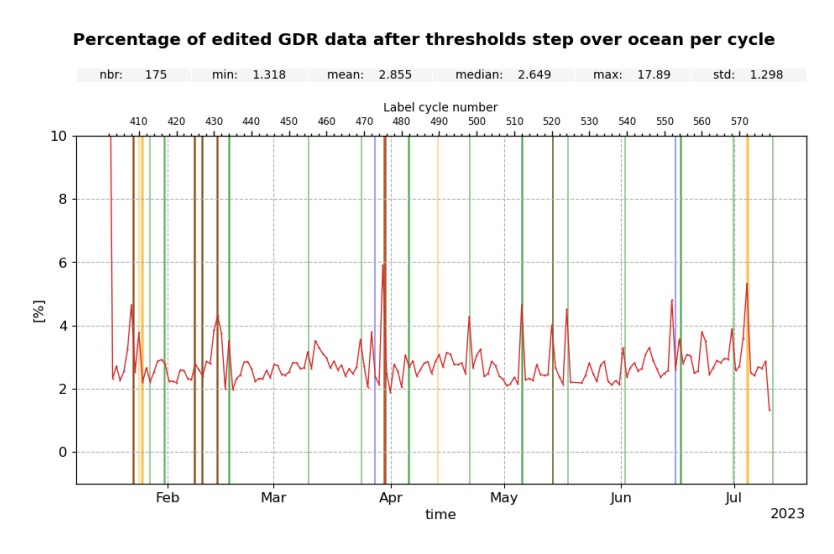


Figure 8: Data editing by thresholds over ocean, average by cycle



Percentage of points edited by thresholds over ocean from C402 to C578

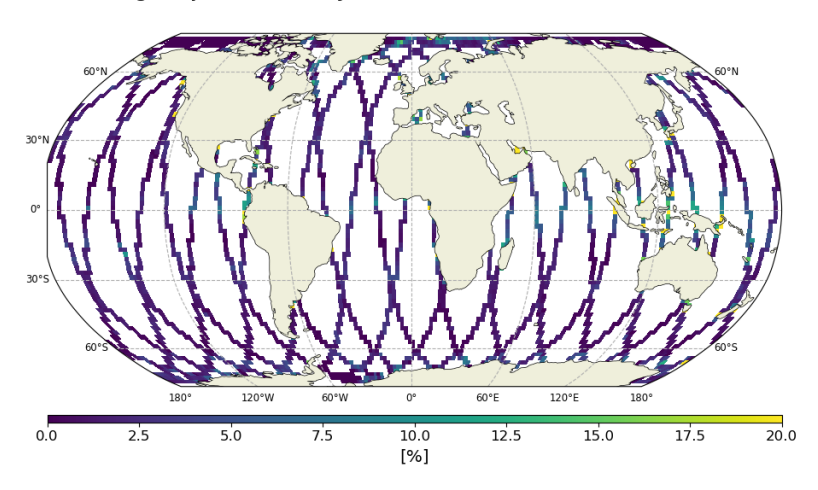


Figure 9: Data editing by thresholds over ocean, map

	Thresholds		
Parameters	Minimum	Maximum	Edited percentage
Sea Surface Height Anomaly (SSHA)	-2 m	2 m	1.80 %
Sea Surface Height (SSH)	-130 m	100 m	0.54 %
Square off nadir angle	-0.2 deg ²	0.64 deg ²	0.49%
Significant Wave Height (SWH)	0 m	11 m	0.52 %
Nb measurements of range	10	20	0.64 %
Std. deviation of range	0 m	0.2 m	1.13 %
Backscatter coefficient (Sigma0)	7 dB	30 dB	0.50 %
Nb measurements of Sigma0	10	20	0.64 %
Std. dev. of Sigma0	0 dB	1 dB	1.17 %
Altimeter wind speed	0 m/s	30 m/s	0.88 %
SSB	-0.5 m	0 m	0.42 %
Ionospheric correction	-0.4 m	0.04 m	0.95 %
Wet Tropospheric Correction (WTC)	-0.5 m	-0.001 m	0.31 %
Dry Tropospheric Correction (DTC)	-2.5 m	-1.9 m	0.00 %
Dynamical Atmospheric Correction (DAC)	-2 m	2 m	0.00 %
Ocean tide	-5 m	5 m	0.00 %
Pole tide height	-15 m	15 m	0.00 %
Earth tide height	-1 m	1 m	0.00 %

Table 6: Table of parameters used for editing.



3.2.3.2 Threshold criteria: 20-Hz range measurements number and standard deviation

1Hz range measurements computed with less than 10 elementary measurements (range_number < 10) are rejected. These are considered as not consistent to compute 1Hz resolution range. Waveforms are distorted by rain cells, which makes them often meaningless for SSH calculation. As a consequence, edited measurements due to several altimetric criteria are often correlated with wet areas. The average percentage of removed measurements using this criterion is 0.64% (Figure 10). They correspond to the peaks visible in Figure 10. Using the threshold editing on 20Hz measurements standard deviation (12), 1.13% of data are removed in average. As for 20Hz range number and std criterion, edited measurements are correlated with wet areas (Figure 13b).

Note that the cycle label tick is drown at the mid cycle datation whereas events are displayed at their real time.

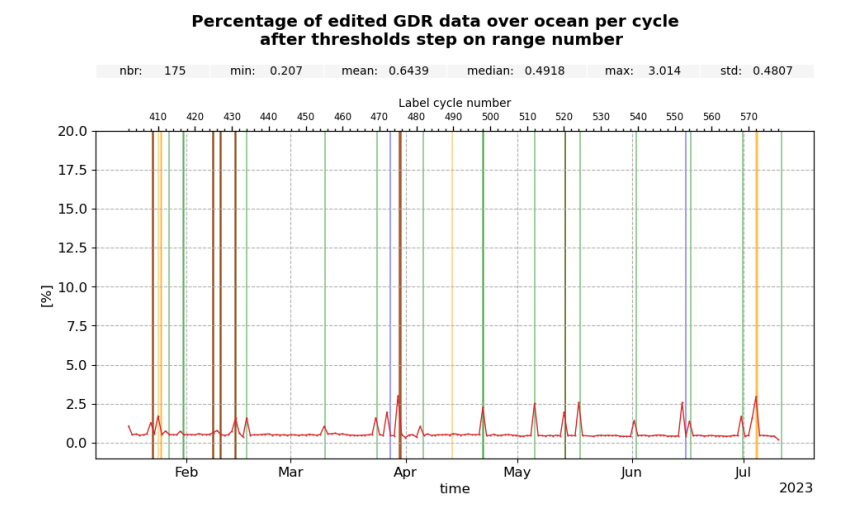
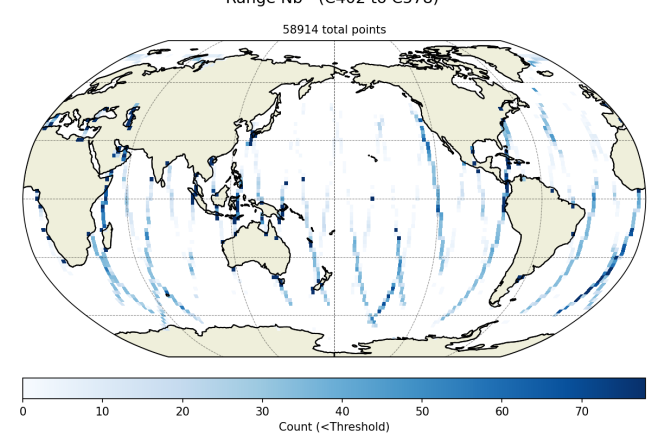
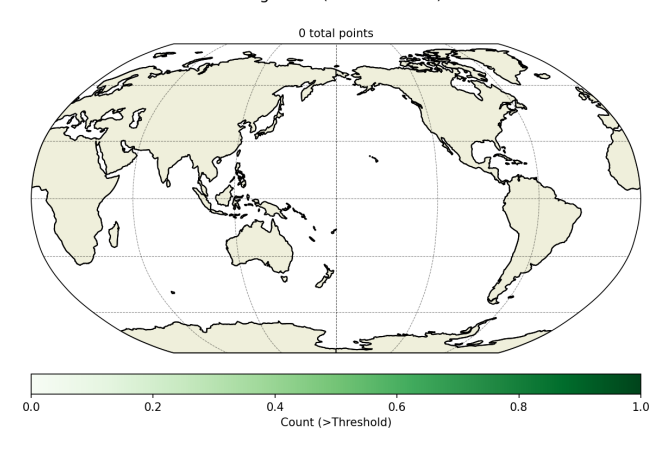


Figure 10: Cyclic monitoring of rejected measurements rate due to range number of 20Hz elementary measurements criterion







(a) Inferior to threshold criteria

(b) Superior to threshold criteria

Geobox count of measurements rejected by thresholds criteria (2°x2°) Range Nb - (C402 to C578)

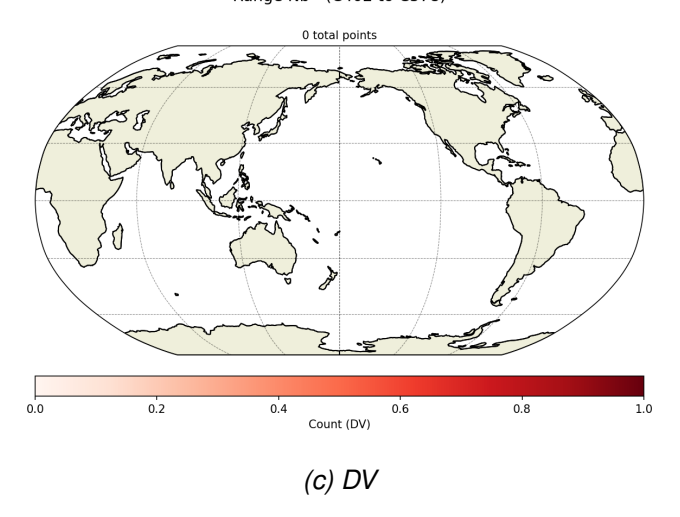


Figure 11: Maps of rejected/discarded measurements due to range number of 20Hz elementary measurements criterion



Percentage of edited GDR data over ocean per cycle after thresholds step on range std

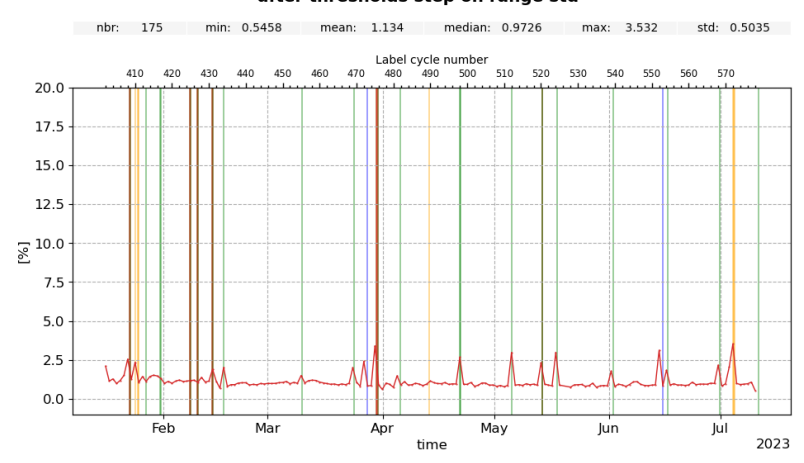
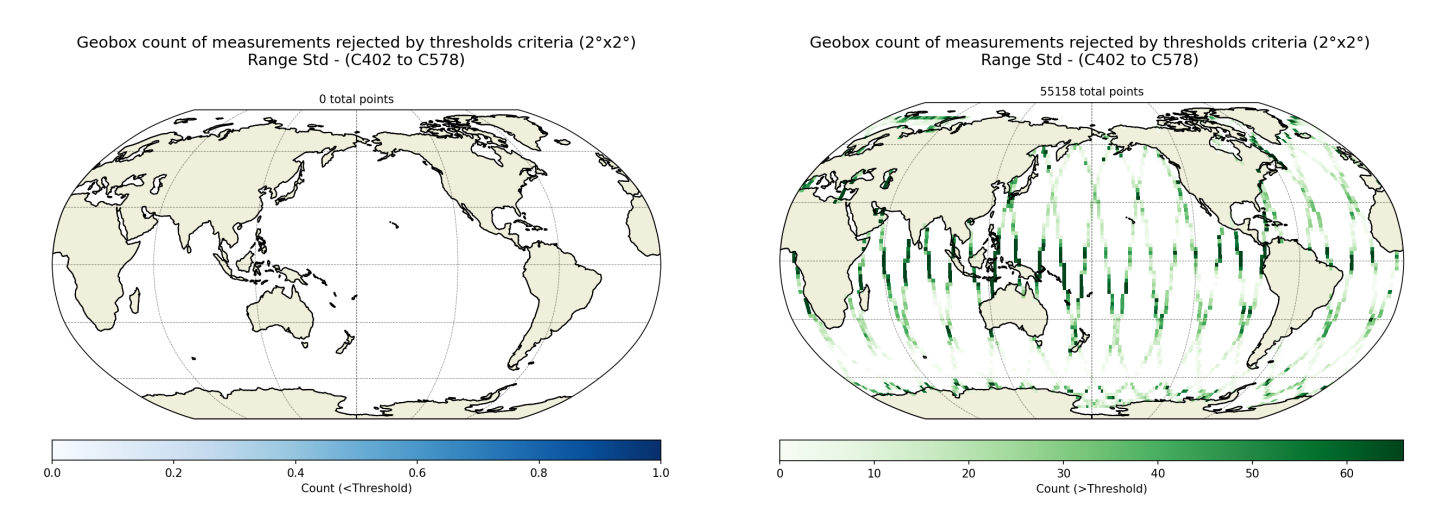


Figure 12: Cyclic monitoring of rejected measurements rate due to range std of 20Hz elementary measurements criterion



(a) Inferior to threshold criteria

(b) Superior to threshold criteria

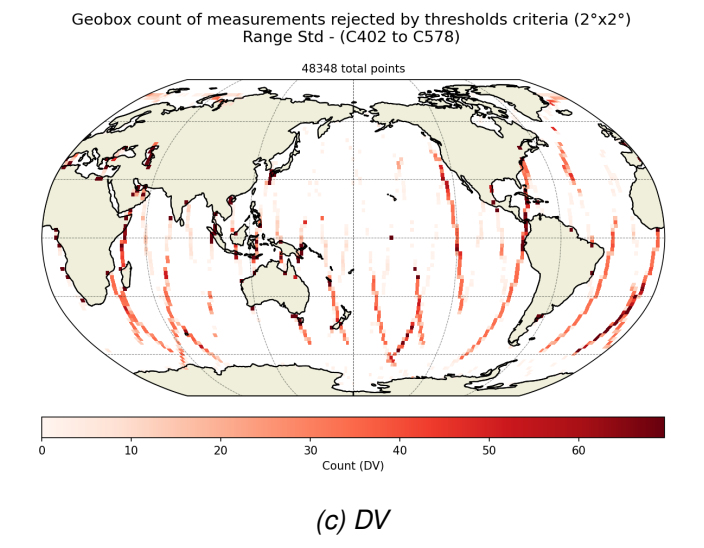


Figure 13: Maps of rejected/discarded measurements due to range std of 20Hz elementary measurements criterion



3.2.3.3 Threshold criteria: Significant wave height (SWH)

The percentage of edited measurements due to significant wave heights criterion is represented in Figure 14, and is about 0.52%. The peaks visible in Figure 14 correspond to the portions of passes at DV visible in Figure 15, they are related to maneuvers as explained in section 2.2.

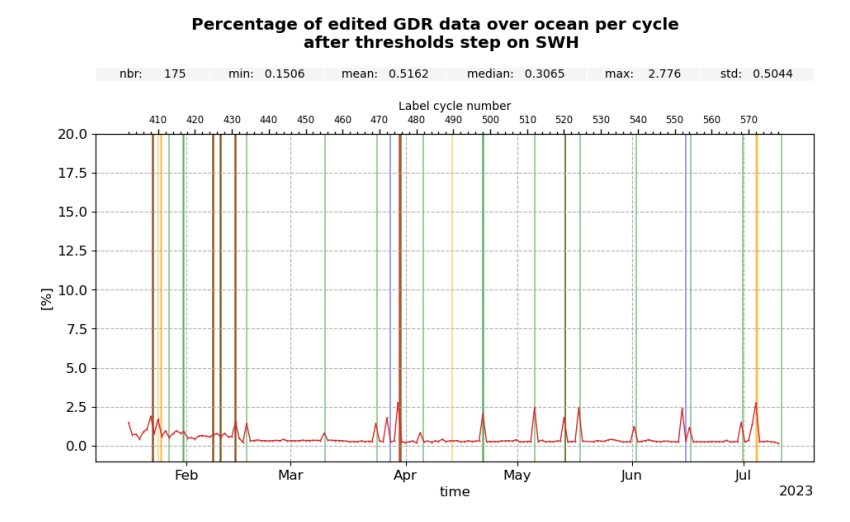
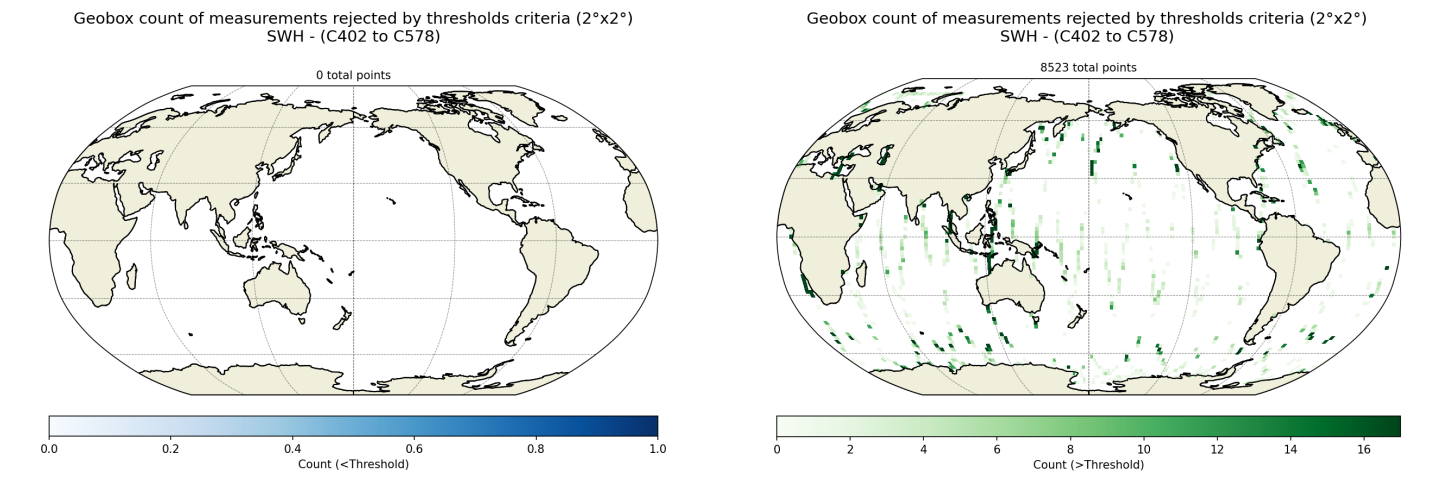
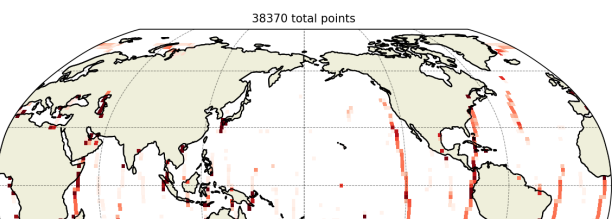


Figure 14: Cyclic monitoring of rejected measurements rate due to SWH criterion



(a) Inferior to threshold criteria

(b) Superior to threshold criteria



Geobox count of measurements rejected by thresholds criteria ($2^{\circ}x2^{\circ}$) SWH - (C402 to C578)

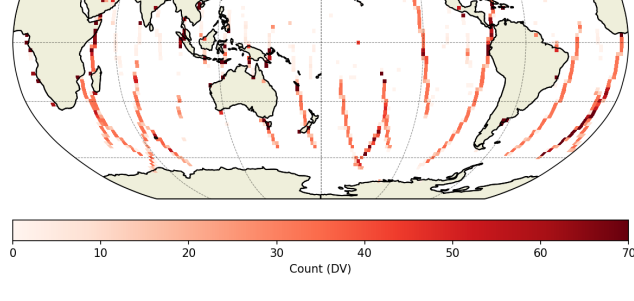


Figure 15: Maps of rejected/discarded measurements due to SWH criterion

(c) DV



3.2.3.4 Threshold criteria: Waveform-derived square off nadir angle

The percentage of edited measurements due to mispointing is about 0.49%. Peaks rejected are always related to maneuvers as explained in section 2.2.

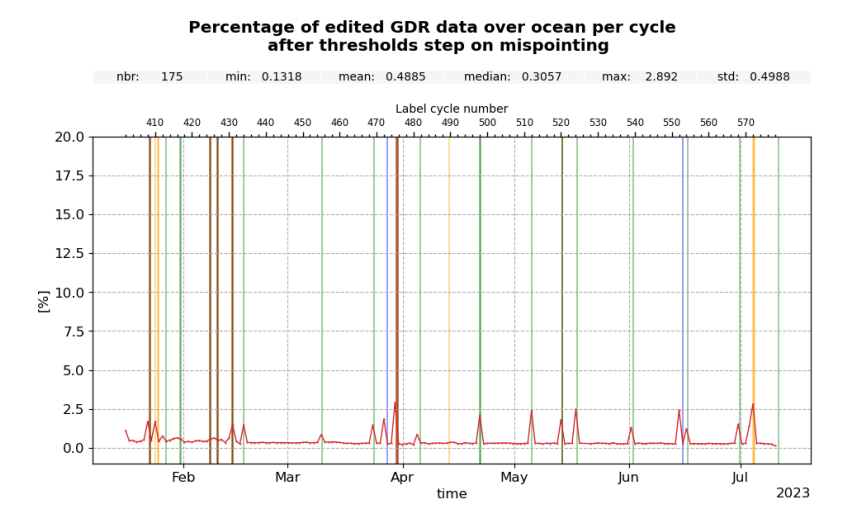
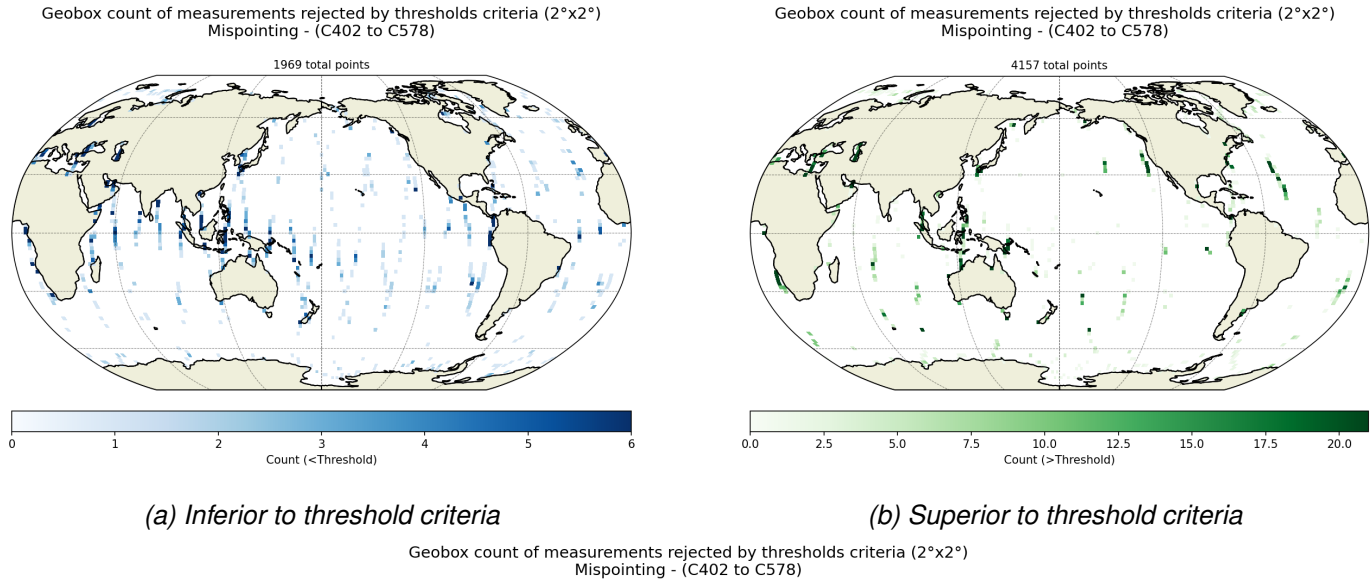


Figure 16: Cyclic monitoring of rejected measurements rate due to mispointing criterion



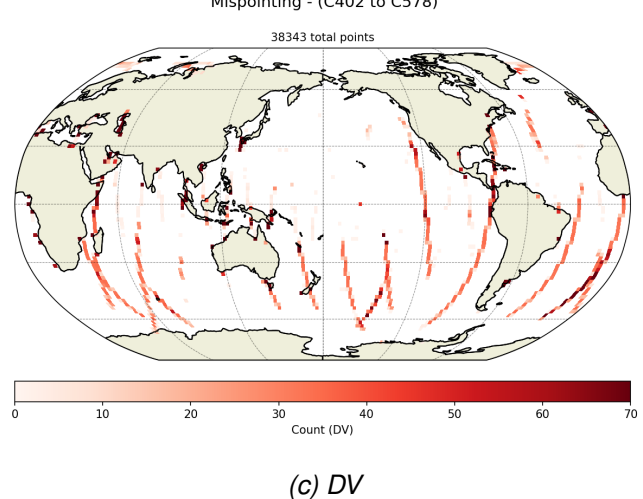


Figure 17: Maps of rejected/discarded measurements due to mispointing criterion

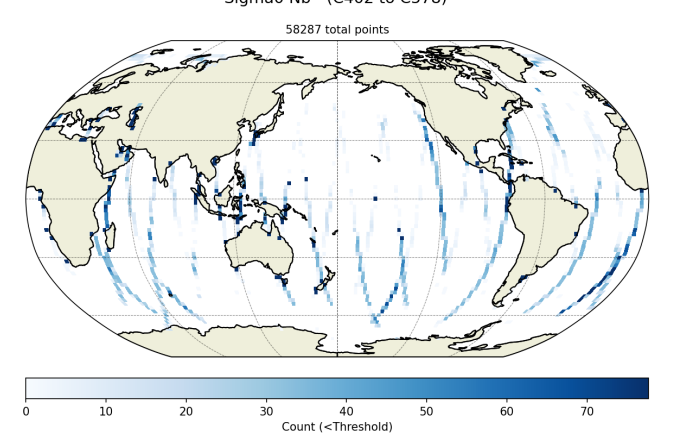


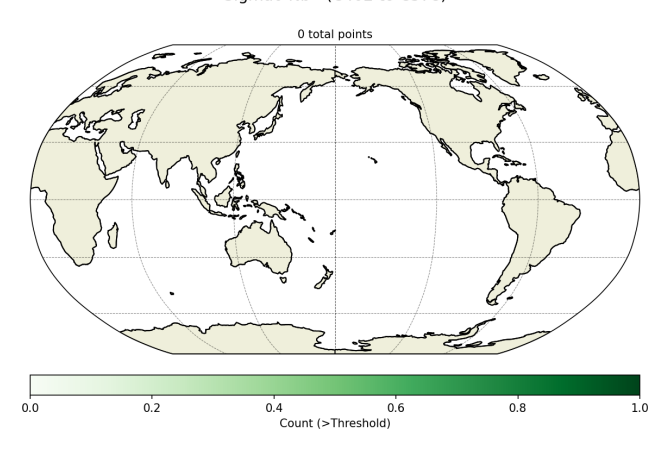
3.2.3.5 Threshold criteria: Sigma0

The percentage of edited measurements due to backscatter coefficient criterion is represented in Figure 18. Peaks rejected are always related to maneuvers as explained in section 2.2.

20Hz Sigma0 number

Figure 18: Cyclic monitoring of rejected measurements rate due to sigma0 number of 20Hz elementary measurements criterion





(a) Inferior to threshold criteria

(b) Superior to threshold criteria

Geobox count of measurements rejected by thresholds criteria (2°x2°) Sigma0 Nb - (C402 to C578)

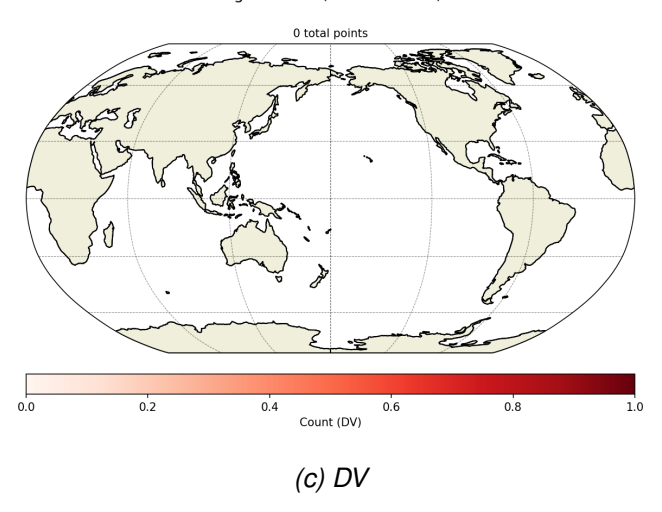


Figure 19: Maps of rejected/discarded measurements due to Sigma0 number of 20Hz elementary measurements criterion



20Hz Sigma0 standard deviation

Percentage of edited GDR data over ocean per cycle after thresholds step on sigma0 std

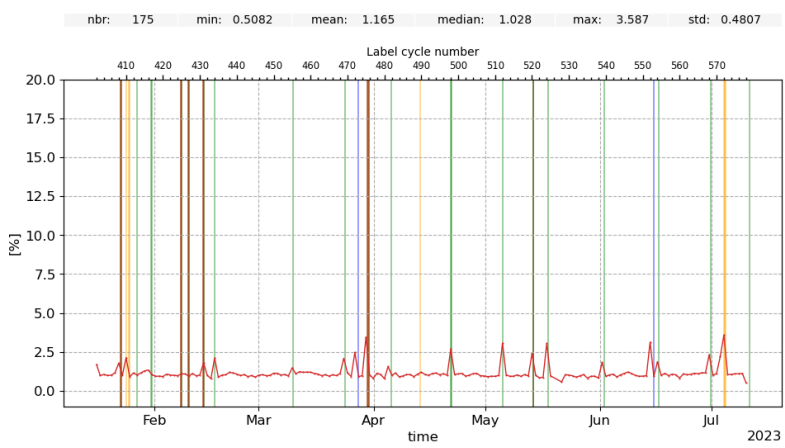
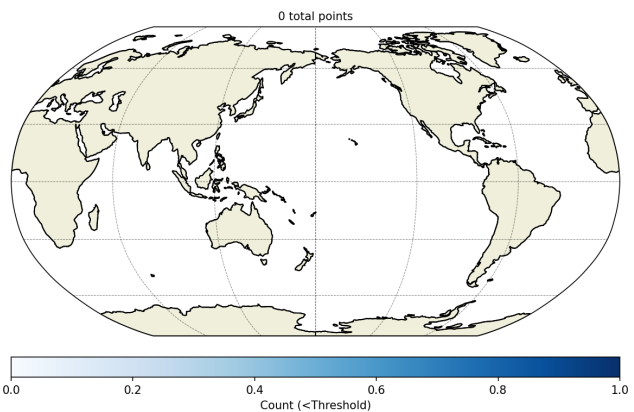
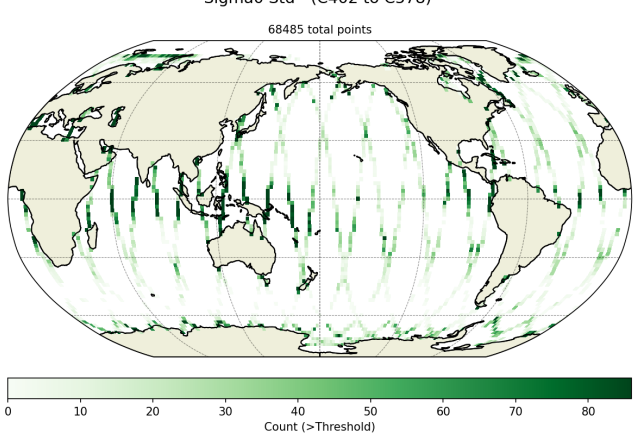


Figure 20: Cyclic monitoring of rejected measurements rate due to sigma0 std of 20Hz elementary measurements criterion

Geobox count of measurements rejected by thresholds criteria (2°x2°) Sigma0 Std - (C402 to C578)



Geobox count of measurements rejected by thresholds criteria (2°x2°) Sigma0 Std - (C402 to C578)



(a) Inferior to threshold criteria

(b) Superior to threshold criteria

Geobox count of measurements rejected by thresholds criteria (2°x2°) Sigma0 Std - (C402 to C578)

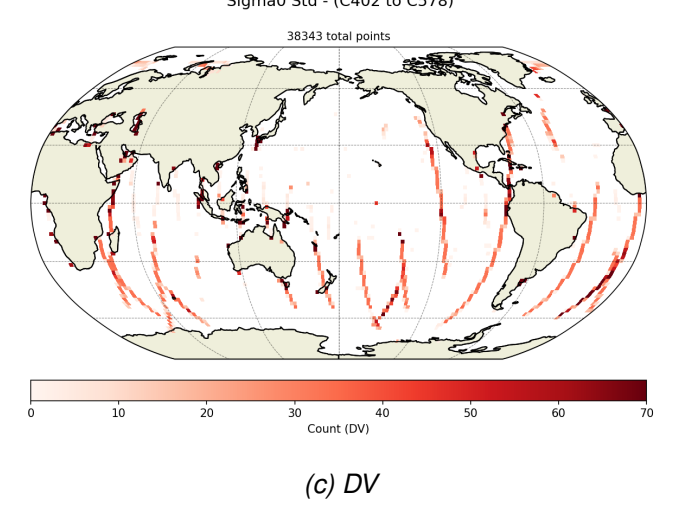
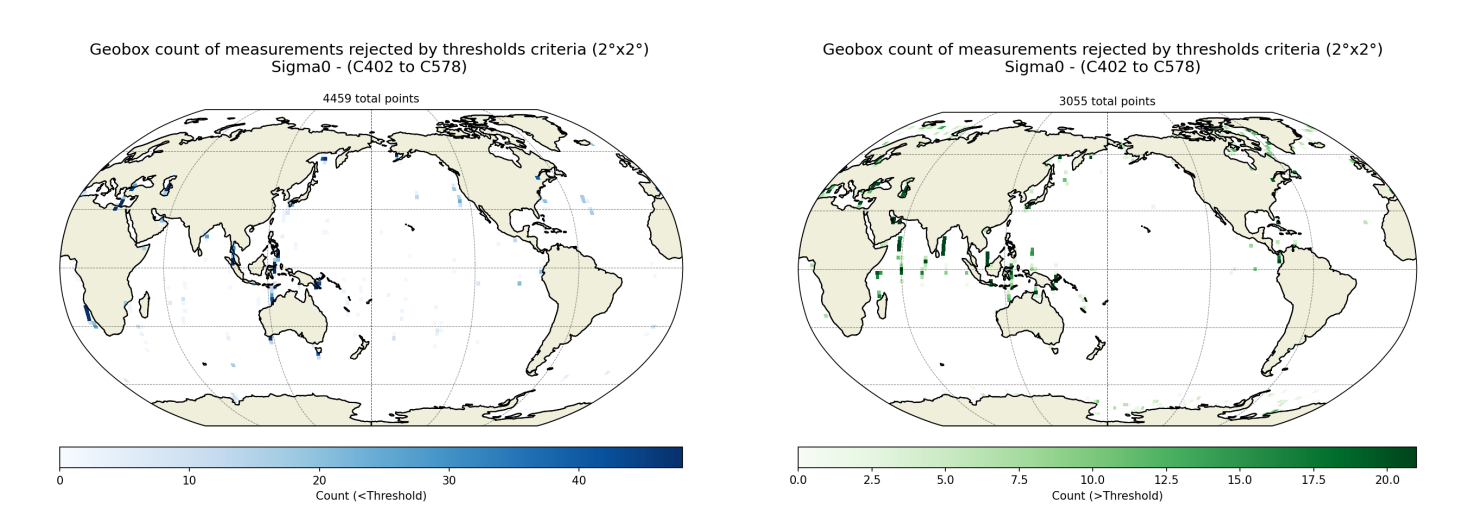


Figure 21: Maps of rejected/discarded measurements due to Sigma0 std of 20Hz elementary measurements criterion



Sigma0

Figure 22: Cyclic monitoring of rejected measurements rate due to sigma0 criterion



(a) Inferior to threshold criteria

(b) Superior to threshold criteria

2023

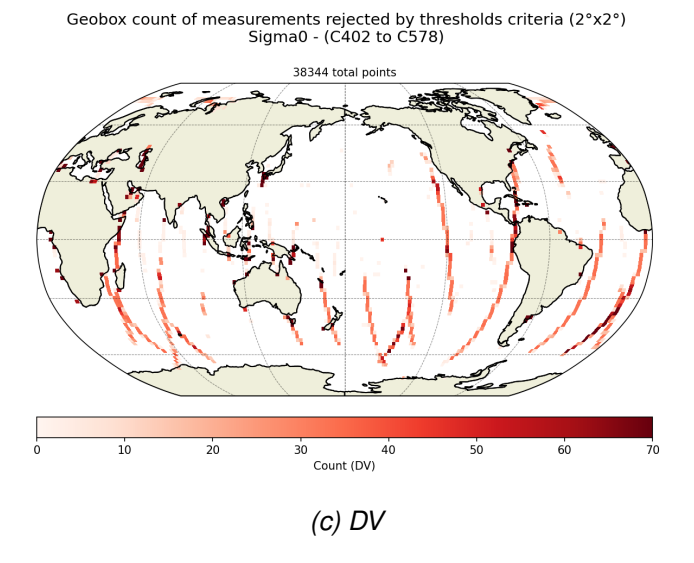


Figure 23: Maps of rejected/discarded measurements due to Sigma0 criterion



3.2.3.6 Threshold criteria: Altimeter wind speed

The percentage of edited measurements due to altimeter wind speed criterion is represented in Figure 24. Measurements are usually edited because of default values (section 2.2). This is the case when sigma0 itself is at default value (as seen in section 2.2), or when it shows very high values (higher than 25 dB), which occurs during sigma bloom situations and also over sea ice. Indeed, the wind speed algorithm (which uses backscatter coefficient and significant wave height) can not retrieve values for sigma0 higher than 25 dB. **Caution:** There are negative altimeter wind speed values in the product but in our internal validation database negative values are set to DV. Nevertheless, sea state bias is available even for negative wind speed values. Therefore, the percentage of edited altimeter wind speed data is higher than the percentage of edited sea state bias data (see part 2.2). The Figure 24 showing percentage of measurements edited by altimeter wind speed criterion is correlated with figures 14 (SWH) and 26 (SSB).

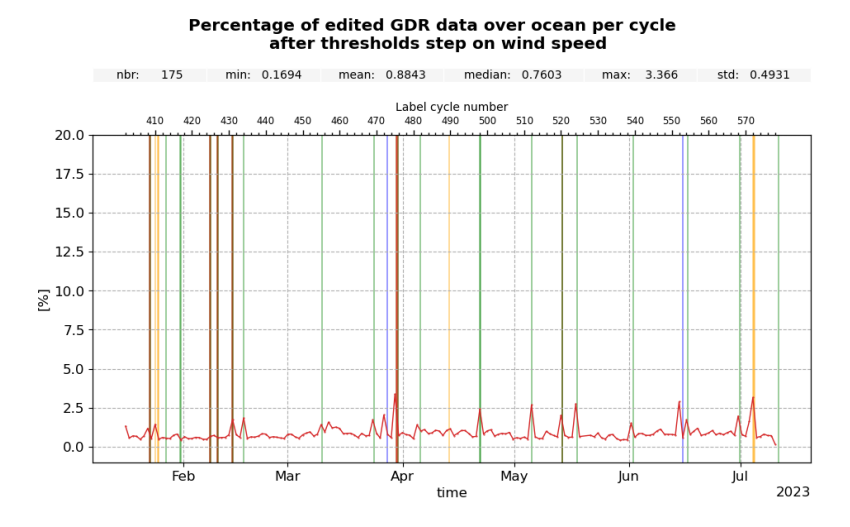
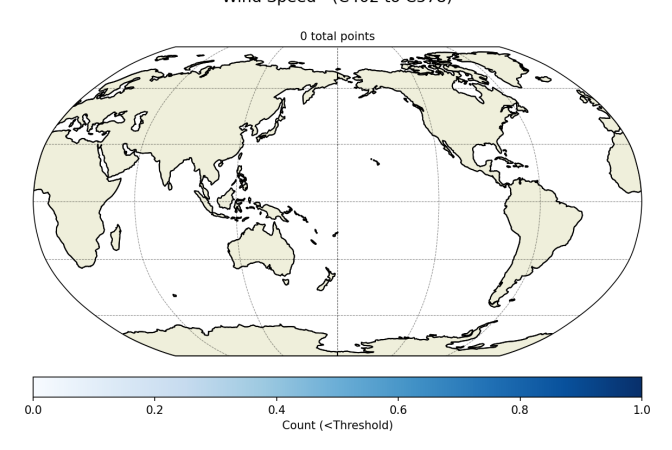
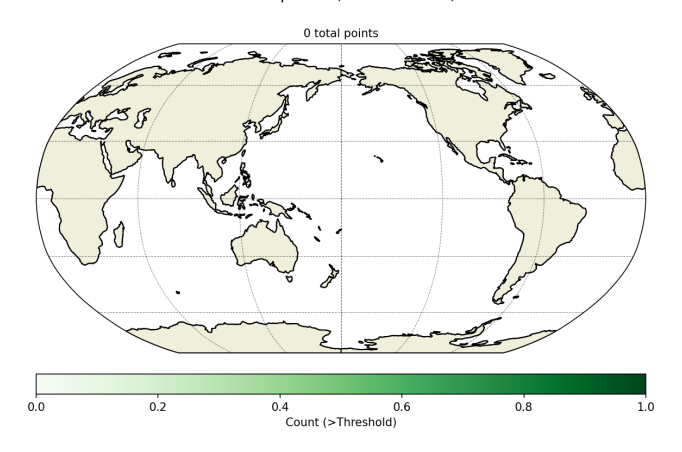


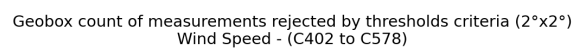
Figure 24: Cyclic monitoring of rejected measurements rate due to Wind Speed criterion





(a) Inferior to threshold criteria

(b) Superior to threshold criteria



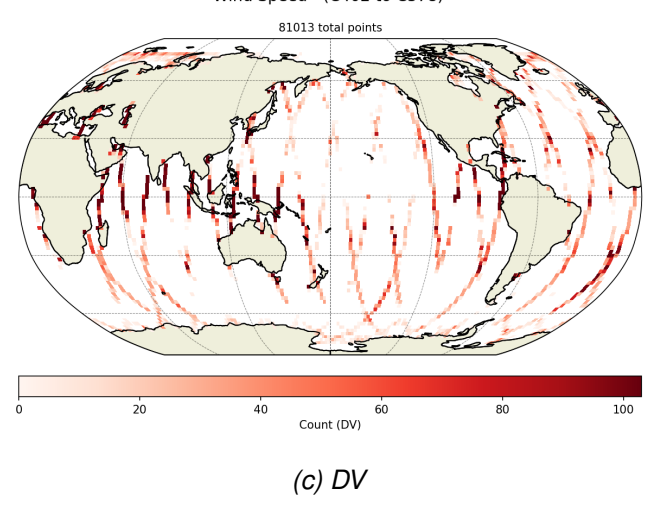


Figure 25: Maps of rejected/discarded measurements due to Wind Speed criterion



3.2.3.7 Threshold criteria: Sea State Bias

Regarding the sea state bias criterion, the percentage of SWOT Nadir edited measurements is about 0.42%. The difference can also be observed on the sigma0 and the significant wave height threshold criteria (which are both used for SSB computation).

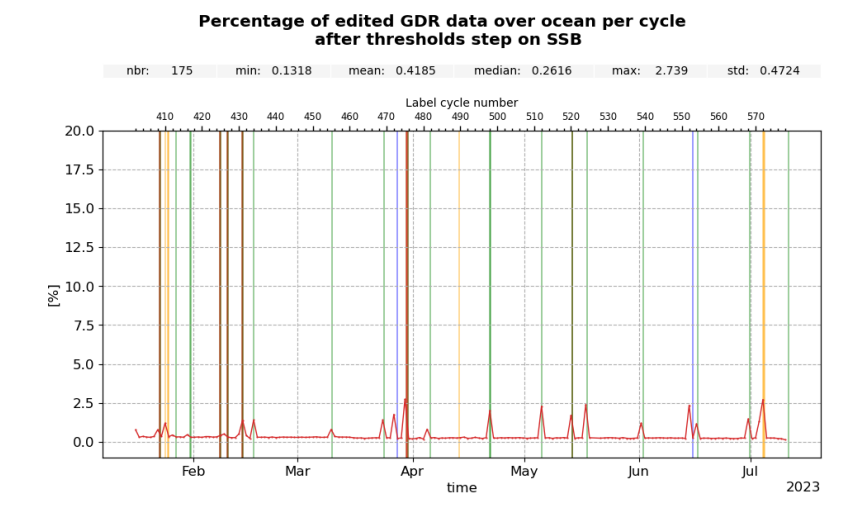


Figure 26: Cyclic monitoring of rejected measurements rate due to Sea State Bias criterion



(a) Inferior to threshold criteria

(b) Superior to threshold criteria

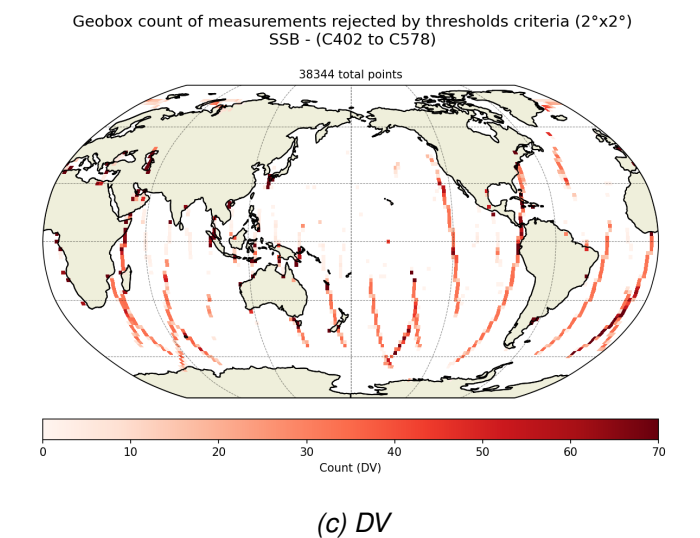


Figure 27: Maps of rejected/discarded measurements due to Sea State Bias criterion



3.2.3.8 Threshold criteria: lonospheric correction

The mean percentage of edited data by threshold criterion on filtered ionospheric correction is 0.95%. The ionospheric correction is computed using combination from Range and SSB (for both Ku and C band)- then a filtering process is applied (as described in section 4.7). As a result, edited points from Range and SSB fields are correlated to edited points from the ionospheric correction. However, due to the filtering of the ionospheric correction small areas of missing SSB and range measurements are filled while some points along the continental coastlines and the Antarctic ice margins are lost.

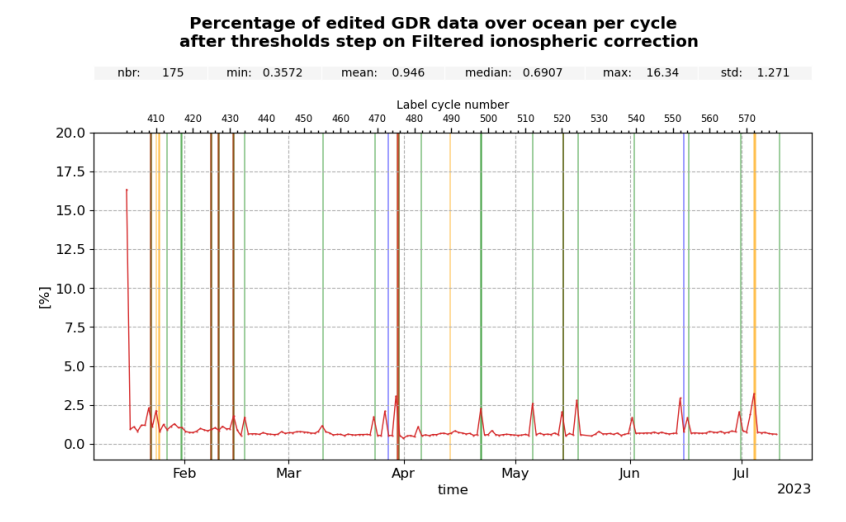
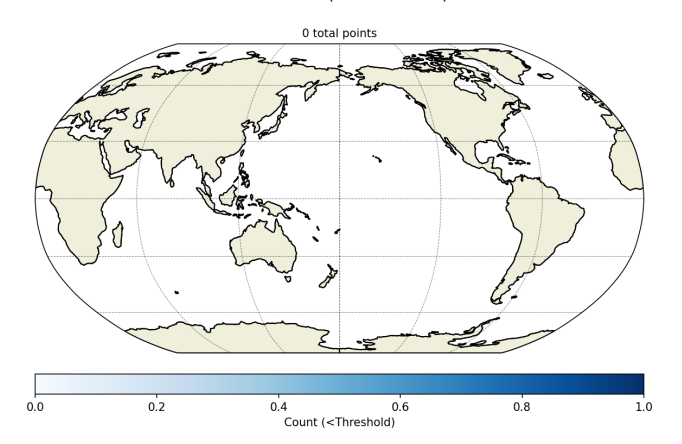
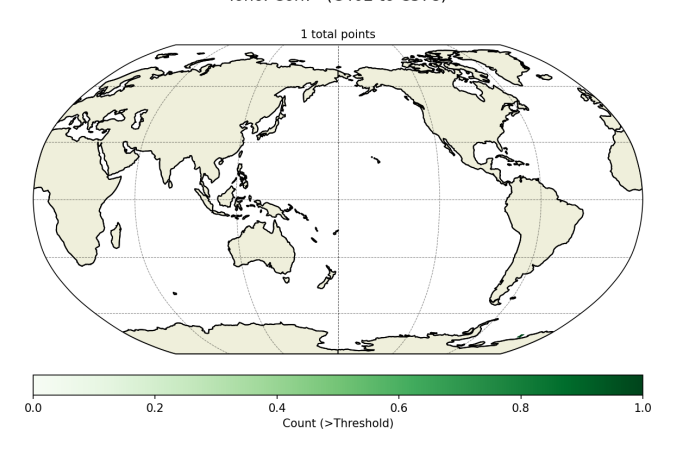


Figure 28: Cyclic monitoring of rejected measurements rate due to ionospheric correction criterion

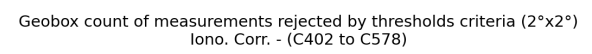






(a) Inferior to threshold criteria

(b) Superior to threshold criteria



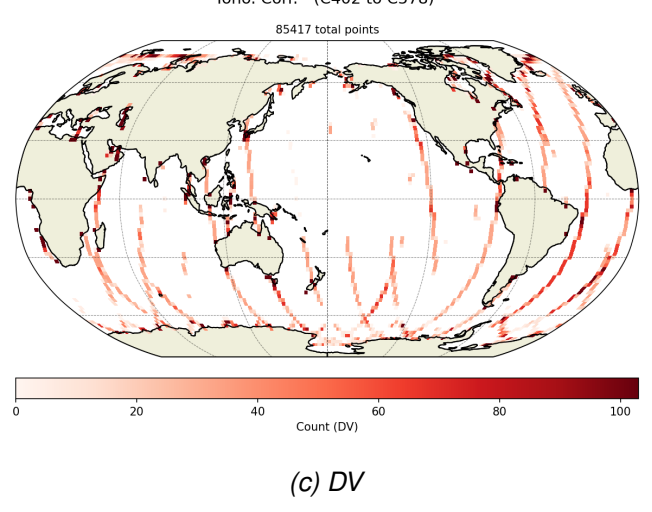


Figure 29: Maps of rejected/discarded measurements due to lonospheric correction criterion



3.2.3.9 Threshold criteria: Radiometer Wet Troposphere Correction

The percentage of edited measurements due to radiometer wet troposphere correction criterion is represented in Figure 30. As for retracking outputs, during maneuvers geolocation problems make interpolation of the 2 radiometers impossible and therefore values are at DV.

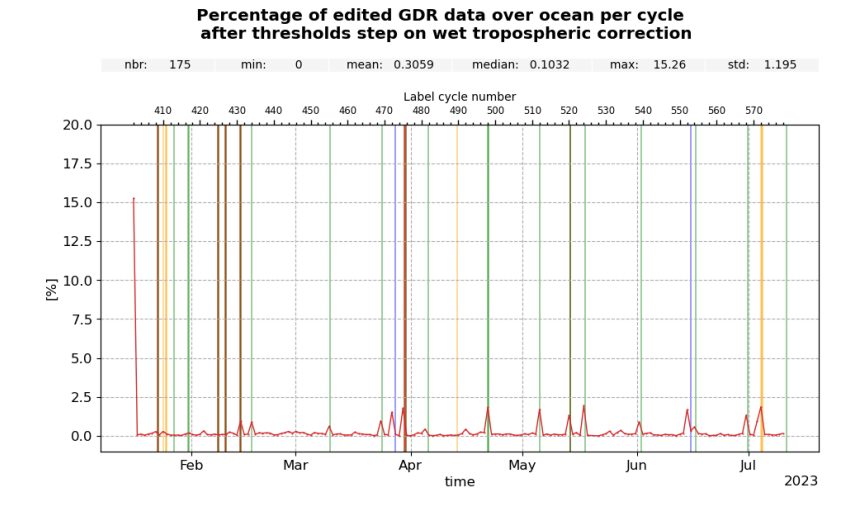
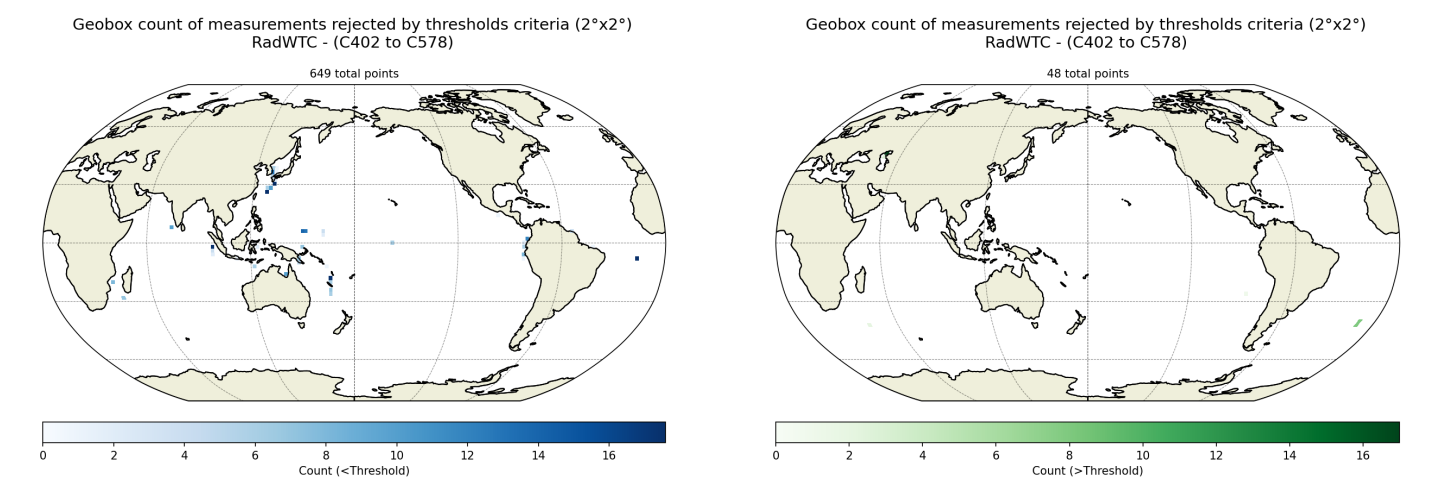


Figure 30: Cyclic monitoring of rejected measurements rate due to Wet Troposphere Correction criterion





(a) Inferior to threshold criteria

(b) Superior to threshold criteria



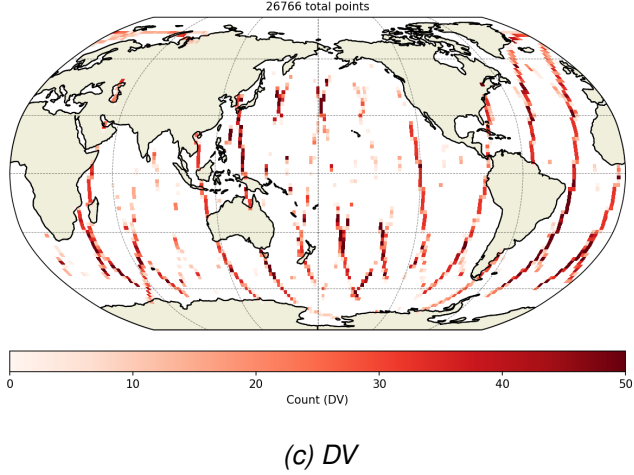


Figure 31: Maps of rejected/discarded measurements due to WTC criterion



3.2.3.10 Threshold criteria: Ocean tide

The percentage of edited measurements due to ocean tide is precisely at 0%. The ocean tide correction is a model output, the few hypothetical edited points would be linked to the coastal interpolation.

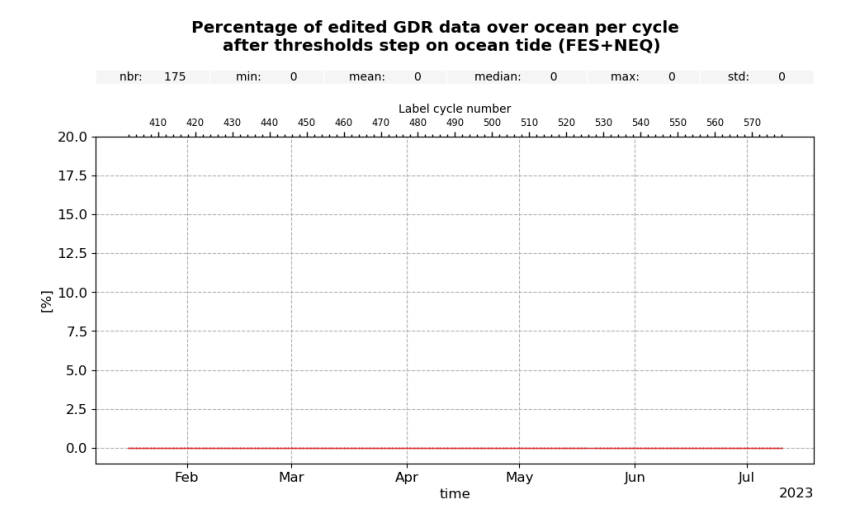


Figure 32: Cyclic monitoring of rejected measurements rate due to ocean tide criterion

3.2.3.11 Threshold criteria: Sea surface height

Sea surface height represents the difference between the orbit and the altimeter range. Figure 33 summarizes the editing resulting from the sea surface height threshold criterion. It removes in average 0.46% of data for SWOT Nadir. The editing is usually due to range measurements at default values near coast in equatorial and mid-latitude regions, as well as regions with low significant wave heights. Moreover, peaks rejected are always related to maneuvers as explained in 2.2.

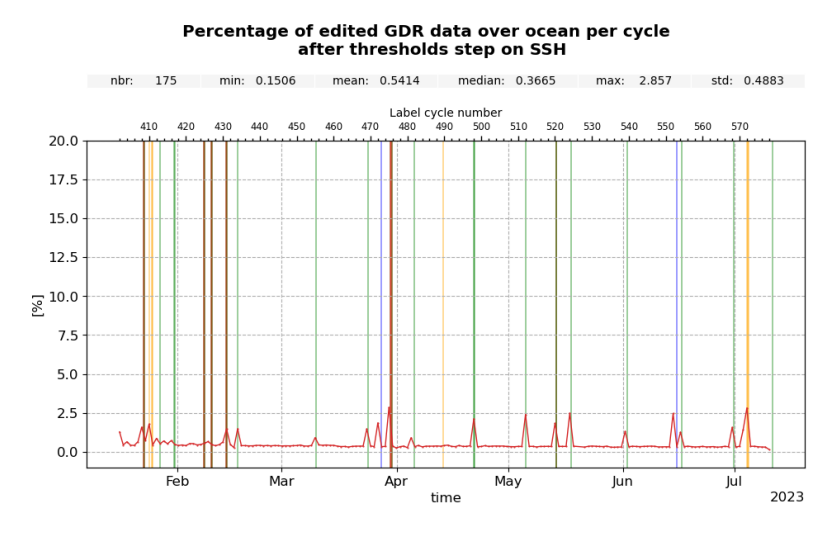
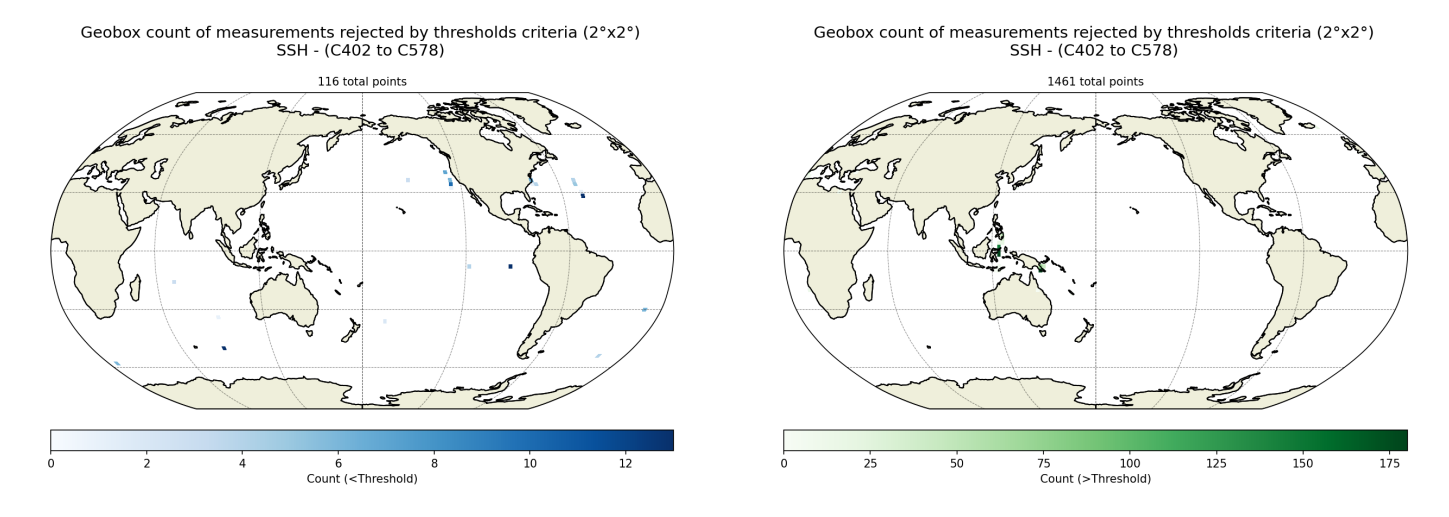


Figure 33: Cyclic monitoring of rejected measurements rate due to Sea Surface Height criterion





(a) Inferior to threshold criteria (b) Superior to threshold criteria

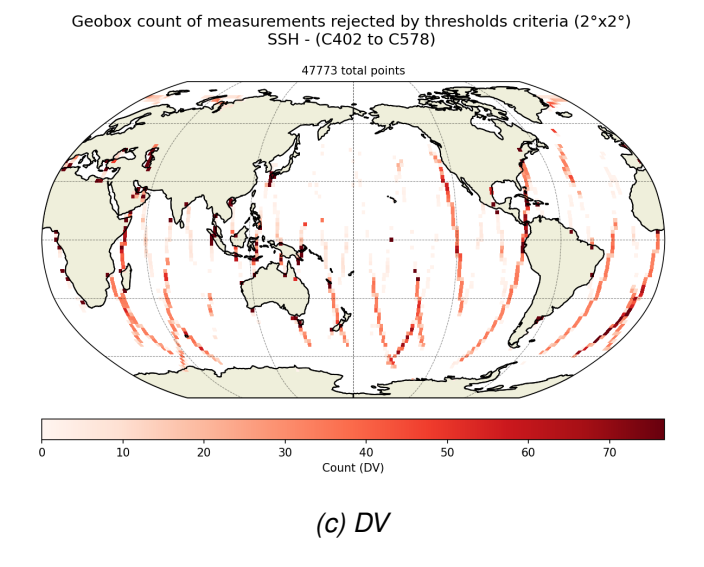


Figure 34: Maps of rejected/discarded measurements due to Sea Surface Height criterion



3.2.3.12 Threshold criteria: Sea Surface Height Anomaly

The percentage of edited data by threshold criterion on SLA is 1.80%. Peaks rejected are always related to maneuvers as explained in section 2.2.

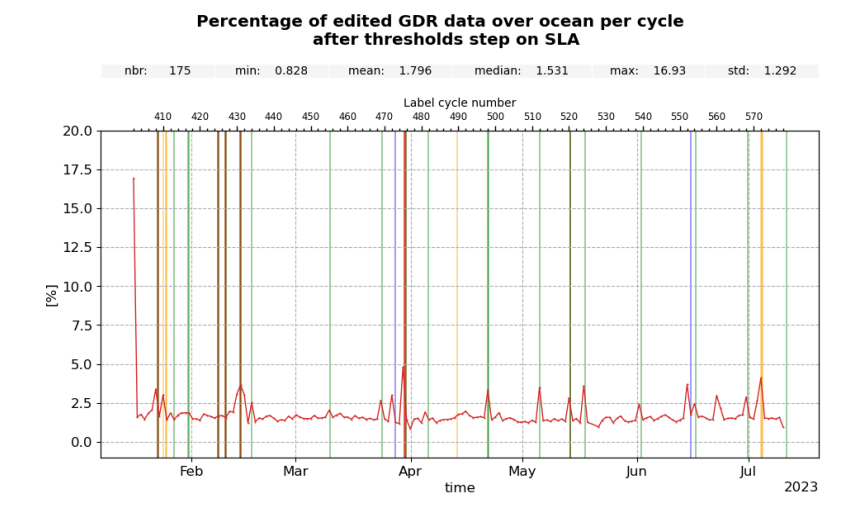
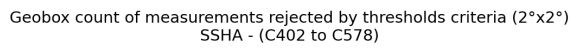
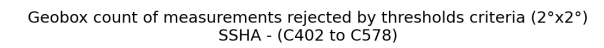
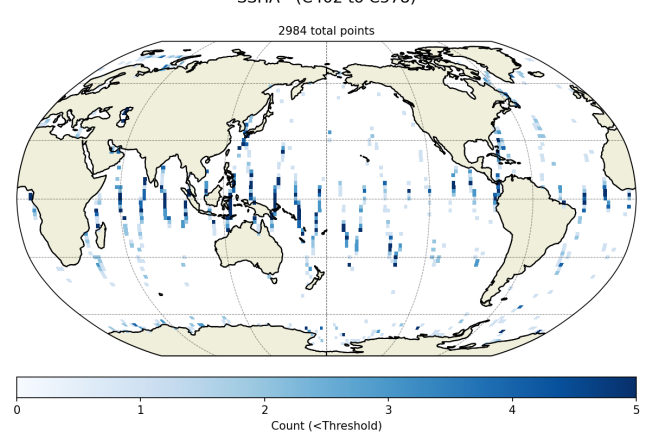


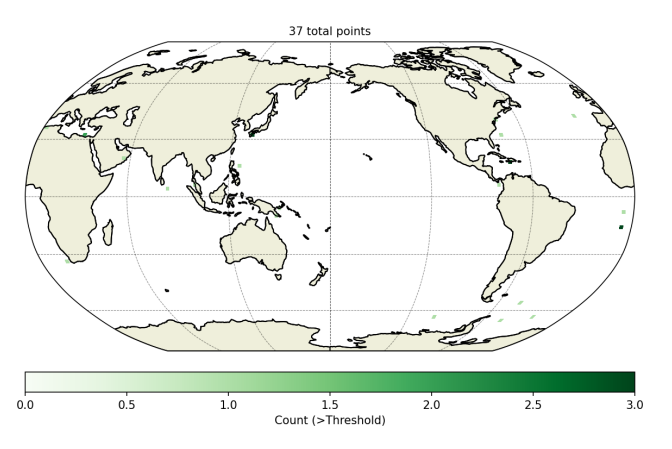
Figure 35: Cyclic monitoring of rejected measurements rate due to Sea Surface Height
Anomaly criterion





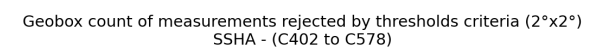






(a) Inferior to threshold criteria

(b) Superior to threshold criteria



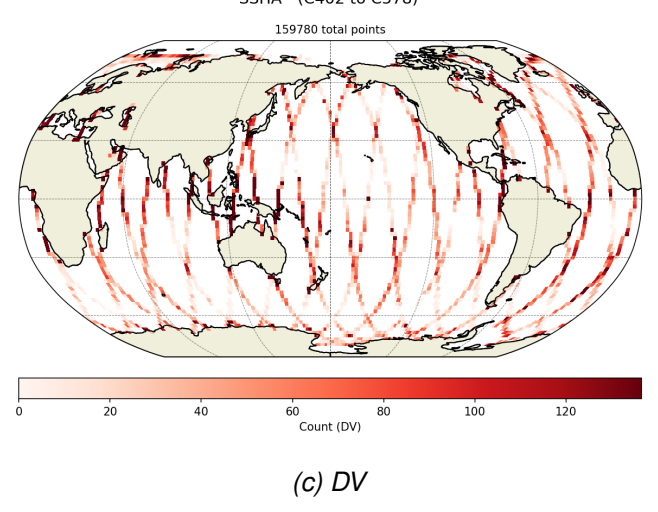


Figure 36: Maps of rejected/discarded measurements due to Sea Surface Height Anomaly criterion



4 Monitoring of altimeter parameters

Note that from this section, we only monitor statistics on valid measurements. Mean and standard deviation of SWOT Nadir main parameters have both been monitored in this report since the beginning of the calval phase.

4.1 20 Hz measurements

The monitoring of the number and standard deviation of 20 Hz elementary range and backscatter coefficient measurements used to derive 1 Hz data is presented here. These two parameters are computed during the altimeter ground processing. As for Jason-3, Jason-2 and Sentinel-6A-MF, before performing a regression to derive the 1 Hz measurements from 20 Hz data, a MQE (mean quadratic error) criterion is used to select valid 20 Hz measurements. This first step of selection consists in verifying that the 20 Hz waveforms can be approximated by a Brown echo model (Brown, 1977 [8], Thibaut et al. 2002 [9]). Then, through an iterative regression process, elementary measurements too far from the regression line are discarded until convergence is reached. Thus, monitoring the number of 20 Hz measurements and the standard deviation computed among them is likely to reveal changes at instrumental level. Standard deviation of range measurements is correlated with significant wave height (SWH dedicated part: 4.3).

The two last purple vertical lines on the right figure (sigma0) correspond to the moments when altimeter was in "INIT" mode the 2023-06-22 from 10:59 to 11:00 (C560 P03) and the 2023-06-23 from 14:16 to 14:19 (C561 P07).

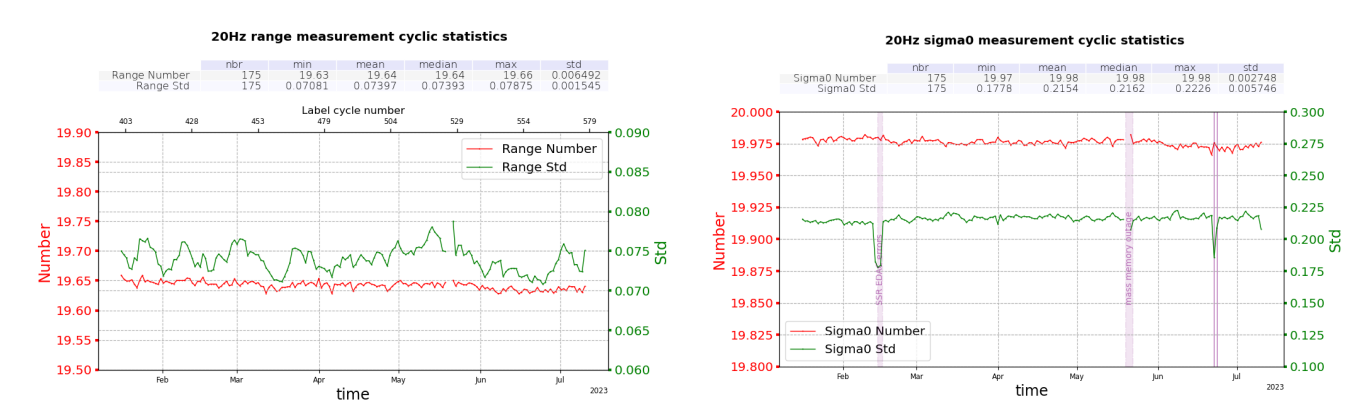


Figure 37: Cyclic monitoring of elementary 20 Hz range and sigma0 measurements



Figure 38 bellow shows the grided statistics of the 20Hz range number and std for the entire period. Range number slightly decreases in regions with ice and in a few coastal regions. In figure 38 right, regions with high 20Hz range variability are associated with regions with strong wave regime.

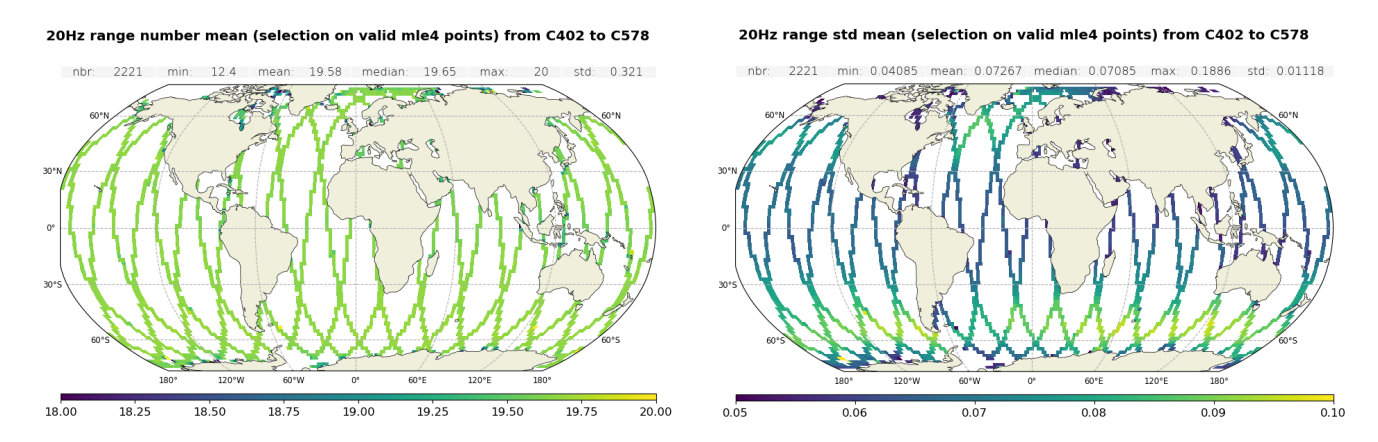


Figure 38: Maps of the 20Hz range measurements, number (left) and std (right).

4.2 Off-nadir angle from waveform

The off-nadir angle is derived from the slope of the trailing edge of the waveform during the altimeter processing: it can either be caused by real platform mispointing or by backscattering properties of the surface. The square of the off-nadir angle, averaged on a cyclic basis (taking into account valid measurements only), has been plotted in Figure 39. The orange vertical lines represent the gyroscope calibrations that occured during the period.

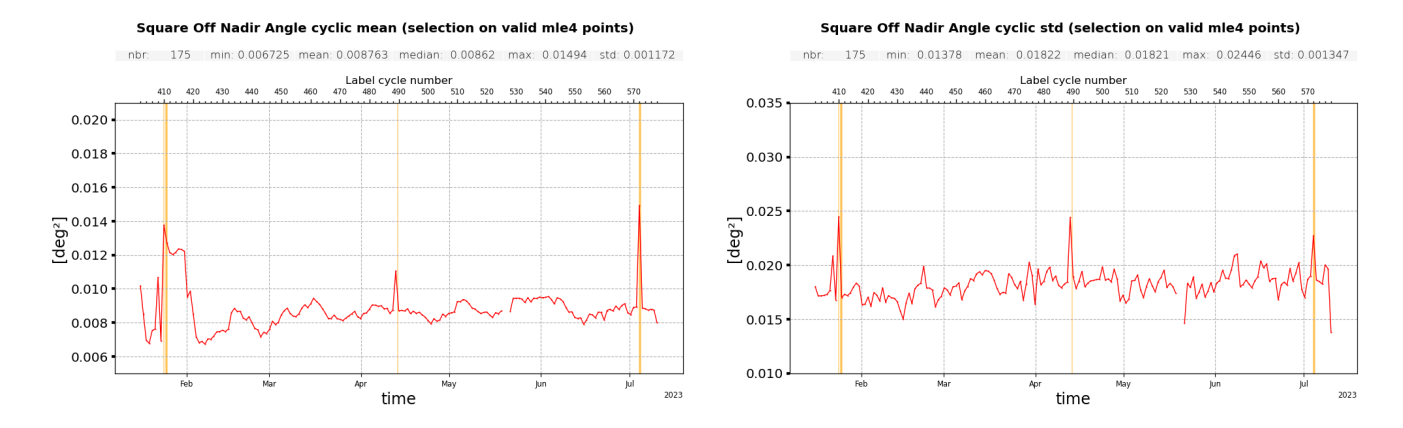


Figure 39: Cyclic monitoring of the square off-nadir angle mean (left) and standard deviation (right).



4.3 Significant wave height

Ku-band wave estimations derived from altimeter measurements are monitored in this section. As shown at the bottom of figure 40 bellow, SWOT Nadir presents a bias of **5.1cm** with regard to ERA5 model.

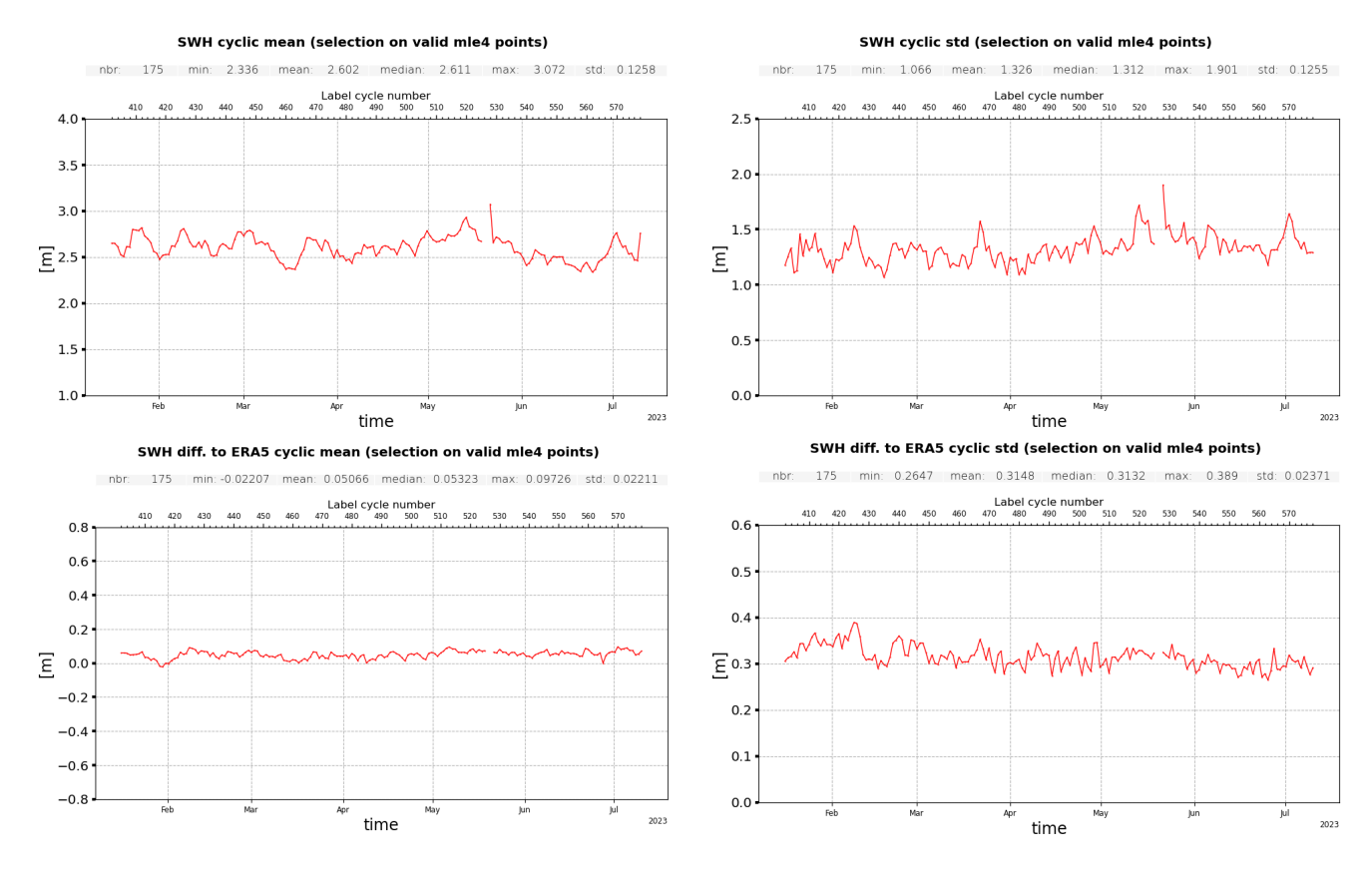


Figure 40: Monitoring of significant wave height (top) and difference to ERA5 swh (bottom). Mean (left) and standard deviation (right).

Figure 41 bellow shows the grided statistics of the difference between SWH MLE4 and SWH from ERA5 model for the entire period. In regions of high wave regimes ($|latitudes| > 30^{\circ}$), SWOT SWH measurements tend to be slighly higher than those estimated by the ERA5 model. A few exceptions, where SWOT SWH measurement are underestimated, occur near the Antarctic.

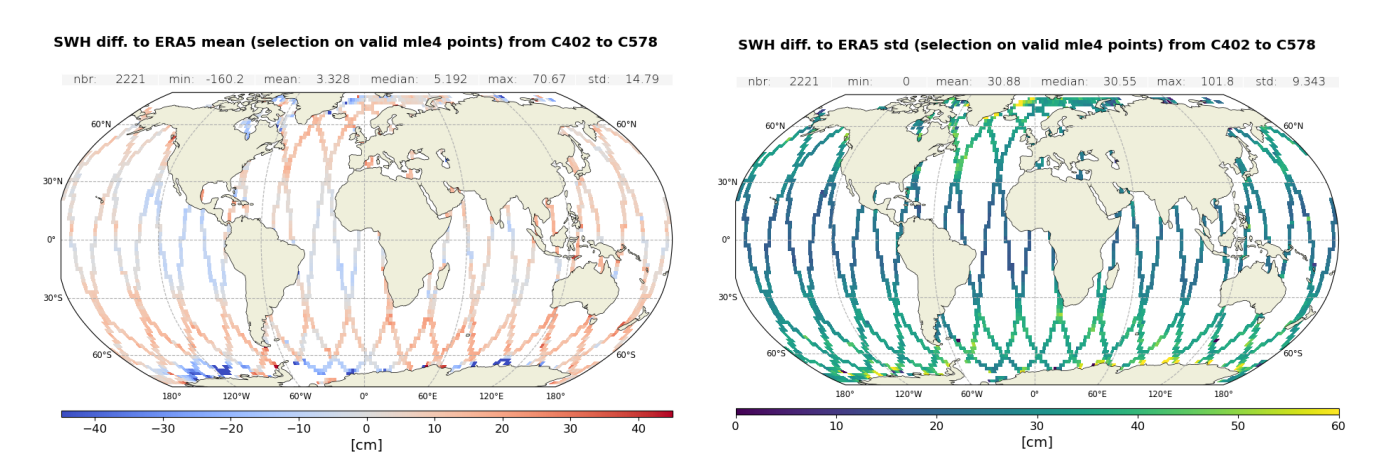


Figure 41: Maps of the SWH MLE4 difference with ERA5 model, mean (left) and standard deviation (right).



The histogram of the SWH distribution for MLE4 and ERA5 model is presented in figure 42 bellow. For SWH from MLE4, the minimal value is 0.233m due to the behaviour of very small wave determination by the retracking. The small bump visible around 0.8m is explained by the waves LUTs used. This problem is also present for Jason-3.

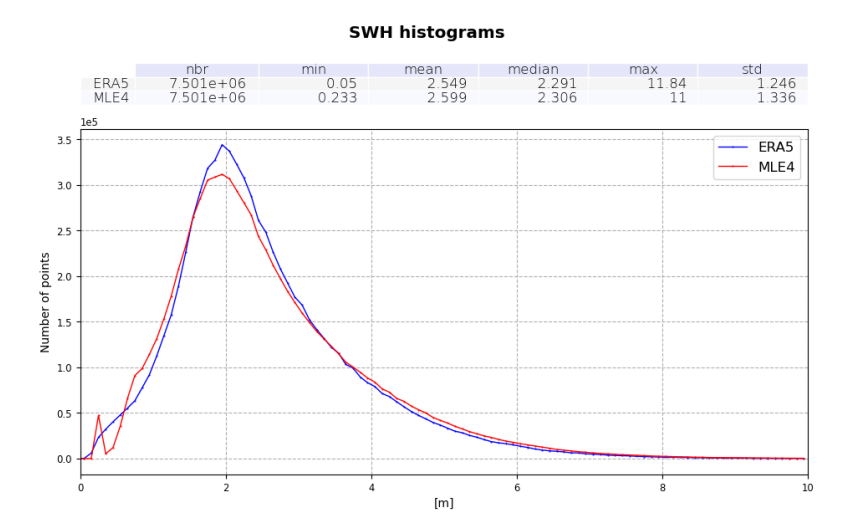


Figure 42: Histogram: SWH ERA5 vs MLE4

4.4 Backscatter coefficient

SWOT Nadir Ku-band backscatter coefficient is stable around 13.47dB for the period (Figure 43).

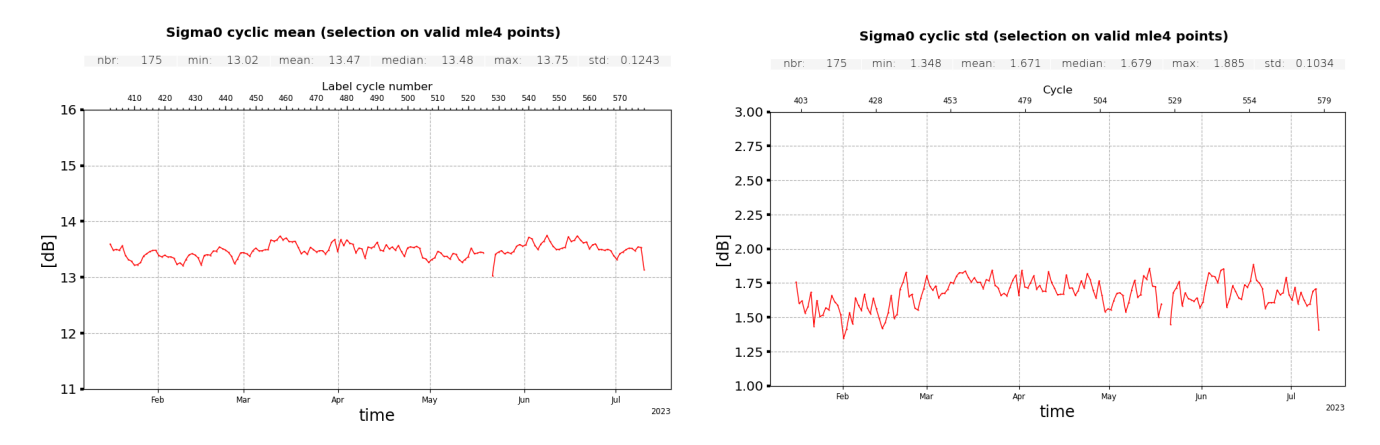


Figure 43: Cyclic monitoring of sigma0 measurements, mean (left) and standard deviation (right).



4.5 Wind speed

Altimeter wind speed is derived from backscattering coefficient and significant wave height using Collard algorithm. To allow wind speed computation, a calibration bias is applied on the backscattering coefficient. The last reprocessing resulted in a jump between GDR-F wind speed and GDR-S2 wind speed of -0.65 m/s. As a result, GDR-S2 wind speed estimations are aligned with ERA5 model with a residual bias of **0.01 m/s** over the entire period (figure 44 bottom).

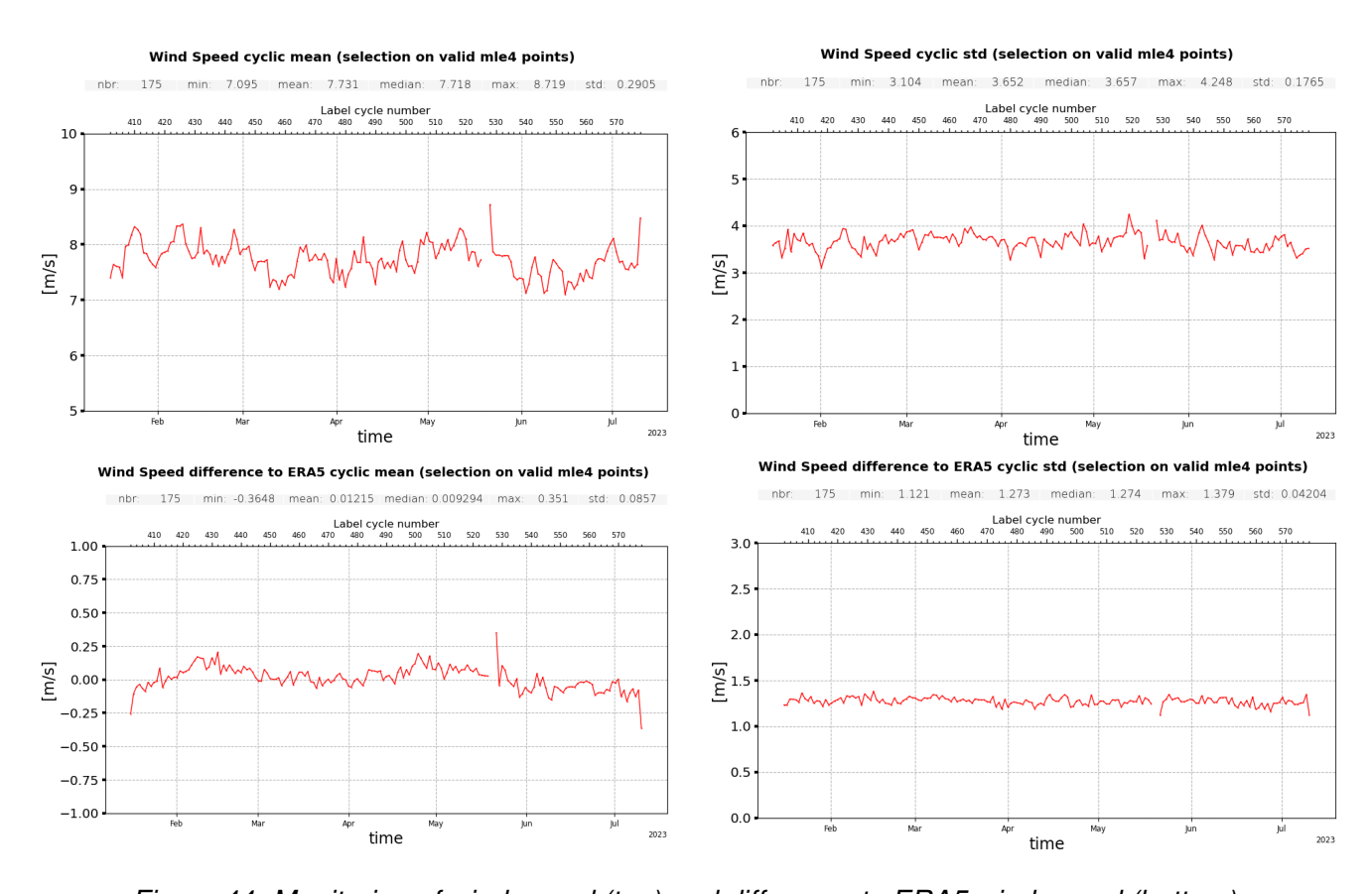


Figure 44: Monitoring of wind speed (top) and difference to ERA5 wind speed (bottom).

Mean (left) and standard deviation (right).



Figure 45 bellow shows the grided statistics of the difference between MLE4 wind speed and ERA5 model wind speed for the entire period.

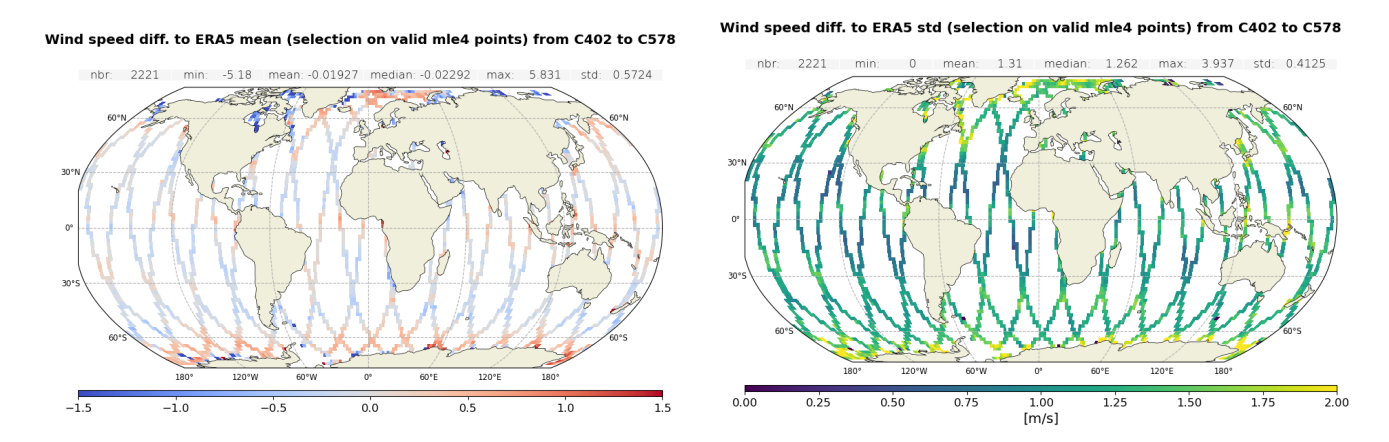


Figure 45: Maps of the wind speed MLE4 difference with ERA5 model, mean (left) and standard deviation (right).

The histogram of the wind speed distribution for MLE4 and ERA5 model is presented in figure 46 bellow.

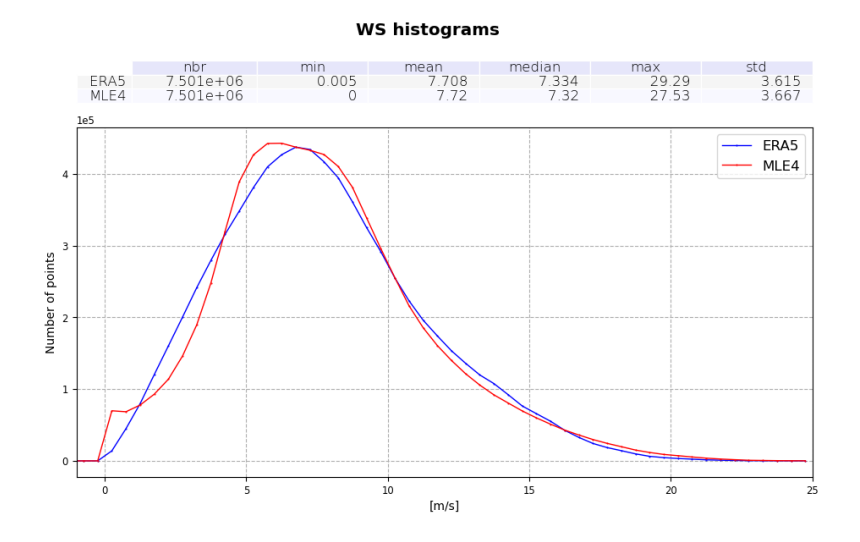


Figure 46: Histogram: Wind speed ERA5 vs MLE4



4.6 Sea State Bias Correction

As mentioned in Section 2.5 SSB table is not fitted to SWOT Nadir data, but the same table as for Jason-3 GDR-F are applied. SWOT Nadir sea state bias mean is centered around -10.05 cm for MLE4 (Figure 47, left), which is consistent with Jason-3 and Sentinel-6A on the same period with -10.04 cm for both missions. SWOT Nadir sea state bias standard deviation is centered around 4.92 cm for MLE4 (Figure 47, right), which is consistent with Jason-3 and Sentinel-6A on the same period with 4.94 cm and 4.93 cm respectively.

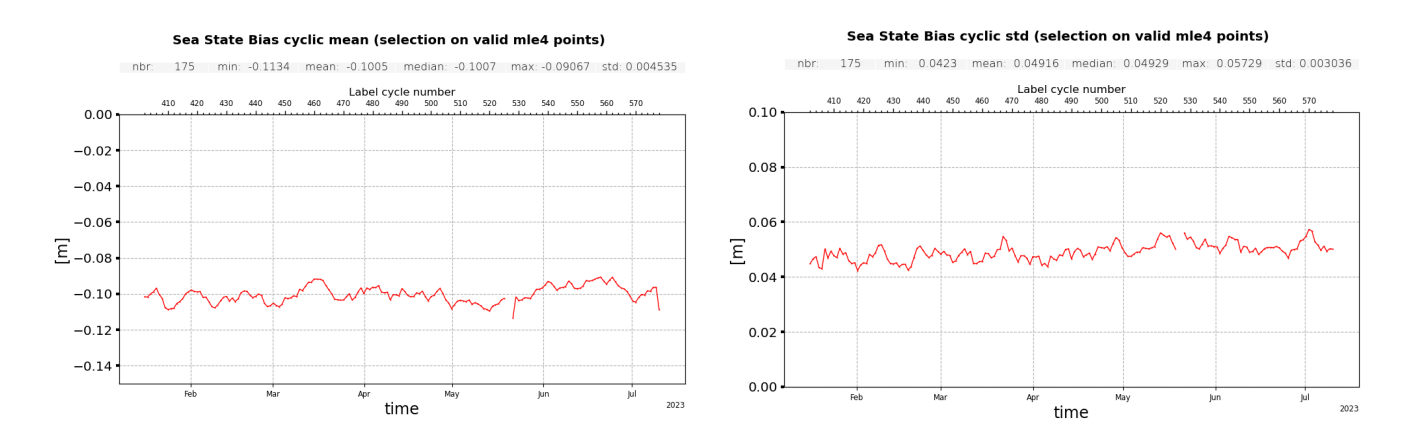


Figure 47: Monitoring of sea state bias

4.7 Ionospheric correction

Note that an iterative filtering method was applied to the ionospheric correction in the production of SWOT Nadir altimetry products. The process is applied to the raw ionospheric correction solution computed from the formula:

$$Iono = \delta f \left[(Range_{Ku} + SSB_{Ku}) - (Range_C + SSB_C) \right]$$
 where $\delta f = \frac{(FrequencyC_{band})^2}{(FrequencyKu_{band})^2 - (FrequencyC_{band})^2}$ represents the frequency factor

For SWOT Nadir, frequency is 5.3 GHz for C-band and 13.575 GHz kor Ku-band. The iterative filtering scheme was developed to achieve two main goals:

- · Base the correction on as many dual-band ionospheric observations as possible
- Improve the correction where altimetric observations are discontinuous or isolated.

This method is fully detailled from Nencioli et al. [10] in Jason-3 GDR-F Reprocessing report [11].

SWOT Nadir mean filtered ionospheric correction is centered around -5.64 cm for MLE4 (Figure 48, left). This is in-line with the missions of reference (Jason-3 and Sentinel-6A) with respectively -5.32 cm and -5.71 cm.

SWOT Nadir standard deviation filtered ionospheric correction is centered around 4.09 cm for MLE4 (Figure 48, right). This is in-line with Jason-3 (4.28 cm) and Sentinel-6A (4.25 cm).

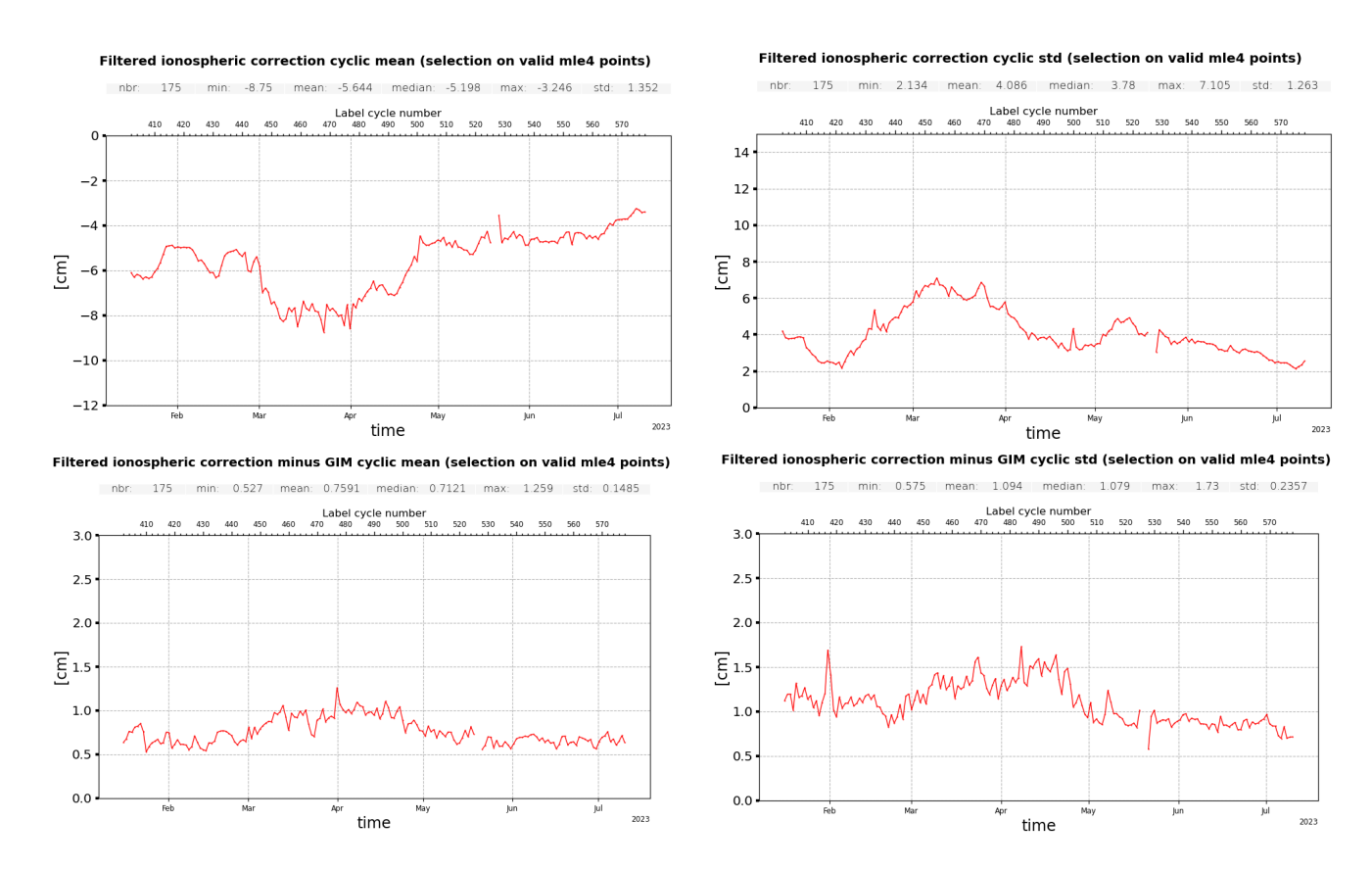


Figure 48: Monitoring of ionospheric correction (top) and difference to GIM iono. corr. (bottom). Mean (left) and standard deviation (right).



The filtering process of the raw signal of ionospheric correction leads, in specific scenario, to a data loss of some points. There are lost because of different causes. The main one is due to the discontinuity in coastal regions. Another cause is a bad behaviour of the algorithm on high variability of the ionospheric correction as shown in Figure 49. The filtering process lost some data points at the extrema of the ionospheric correction. The cause of this behaviour is not yet fully understood, and a study is currently ongoing to investigate it.

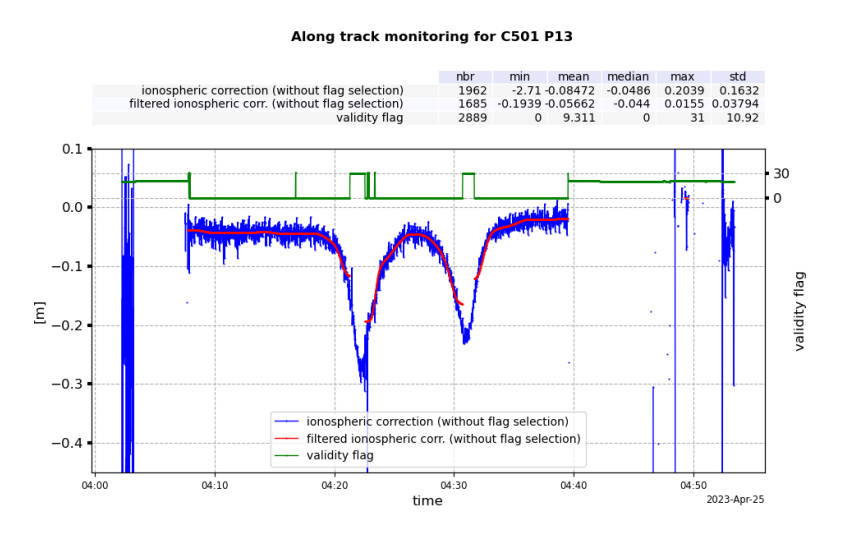


Figure 49: Along track monitoring of ionospheric correction for C501 P13

Figure 50 illustrates the percentage per cycle of ionospheric correction lost measurement by filtering and figure 51 illustrates the distribution of this lost points. The passes that are fully lost over ocean are passes 5 to 8 from cycle 402. For these passes there was no radiometer data available, hence there is no available information for *surface_classification_flag* and nor for sea_ice_flags. Since those flags are mandatory for the computing of ionospheric correction it explains the absence of ionospheric correction measurements. The figures clearly show that the majority of points are lost in coastal area and only represents a small fraction of ionospheric correction points.

The statistics are computed as follow: a selection over ocean is done with *surface_classification_flag=0*; a measure is considered lost if *iono_cor_alt_filtered* is at default value while *iono_cor_alt* is not at default value.

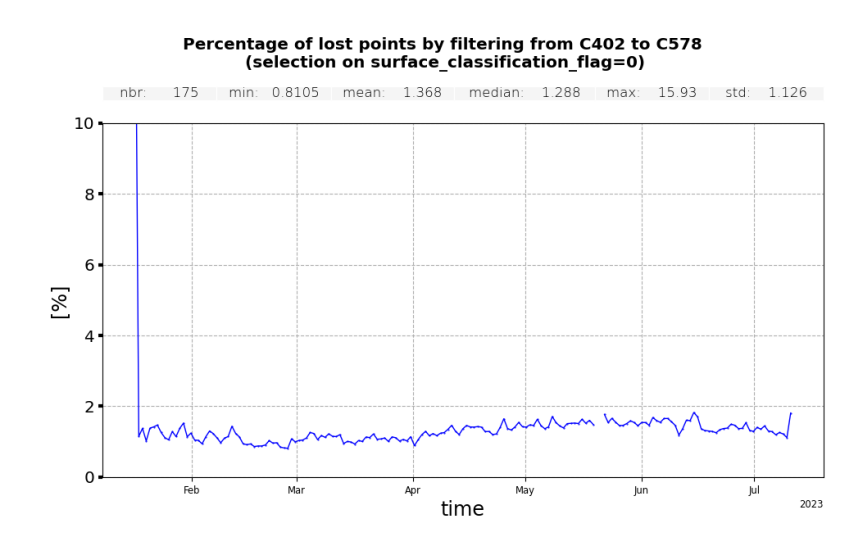


Figure 50: Temporal monitoring of ionospheric correction measurements lost by filtering



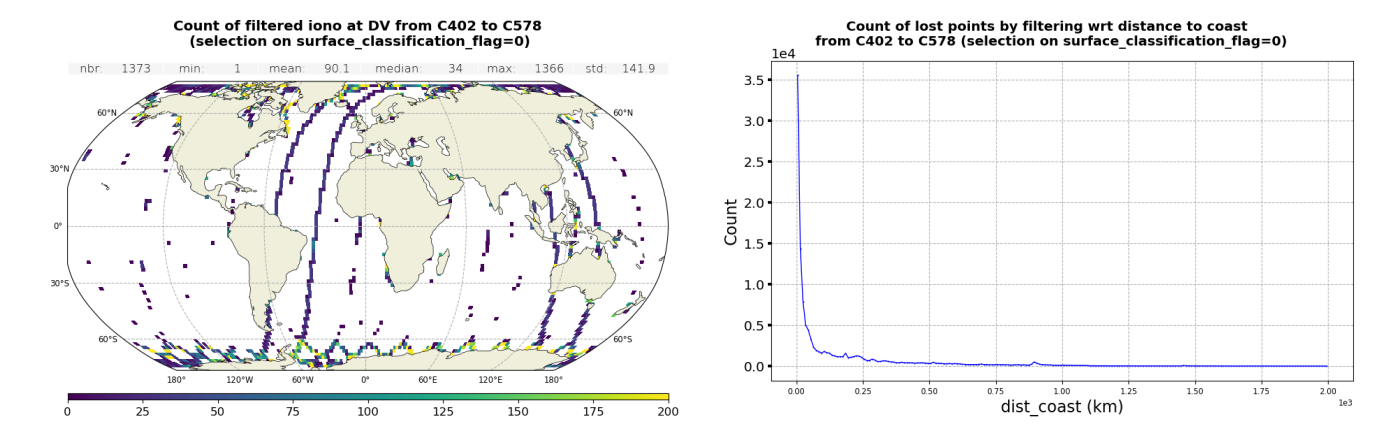


Figure 51: Monitoring of lost ionospheric correction points through filtering

5 Validation and Monitoring of Radiometer Parameters

5.1 Geophysical products monitoring

For the SWOT mission, the Wet Tropospheric Correction is measured by a radiometer with two independants beams, measuring tropospheric correction on each sides of Nadir, with AMR Side 1 35 km away from Nadir, and Side 2 40 km away. Depending of Yaw Flip, one beam measures the Wet Tropospheric Correction slightly fore of the Nadir Altimeter measurement, while the other beam measure aft of Nadir Altimeter measurement. Then, an interpolation using the two radiometer sides is performed to obtain the Wet Tropospheric Correction on each 1Hz altimeter measurement.

Figure 52 shows the evolution of the Wet Tropospheric Correction measured by the radiometer (on both sides) and interpolated at the Nadir, for all points where both the interpolated WTC and the closest S1/S2 radiometer points are valid. This ensures a consistent selection across all datasets. Some variations can be seen, mainly due to seasonal effects.

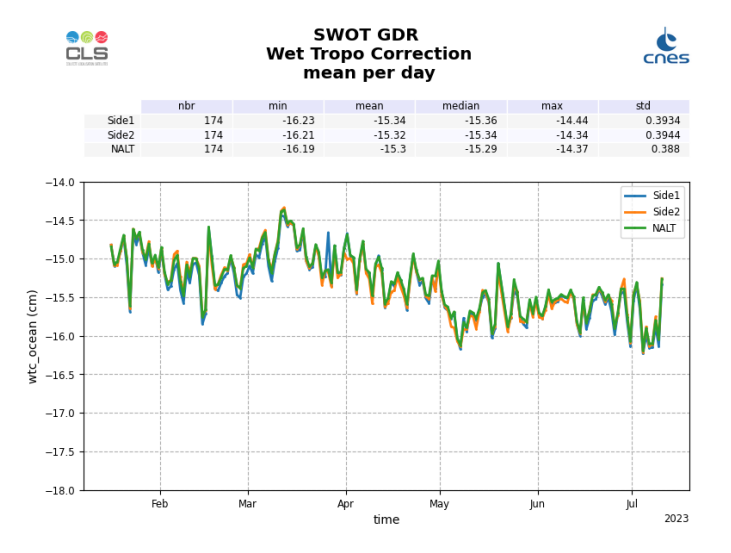


Figure 52: Daily monitoring of the mean of the Wet Tropospheric Correction for the AMR S1 (blue), AMR S2 (orange) and Nadir (green) for the entire calval phase

To assert the quality of the WTC from the satellite, it is compared to a WTC computed from the ECMWF operational model, available every 6 hours, with a resolution of 0,25 degree. The WTC from model is then linearly interpolated at radiometer measurements locations for both sides and Nadir measurements locations. Figure 53 shows the evolution of the daily mean and standard deviation of the difference between WTC derived from AMRs and WTC derived from model, for both AMRs beams and Nadir. This shows the stability of SWOT's WTC as mean varies under 1mm. Also, it shows the good alignment between the two radiometer sides and the Nadir on the GDR-S2 dataset as the difference is almost identical for the three. The daily standard deviation is stable too, around 1.1 cm for the radiometer, which is the nominal standard deviation expected (similar to Jason -3 and Sentinel-6). The daily standard deviation of the difference is only 0.9 cm for the Nadir interpolated WTC, due to the smoothing effect of the interpolation.



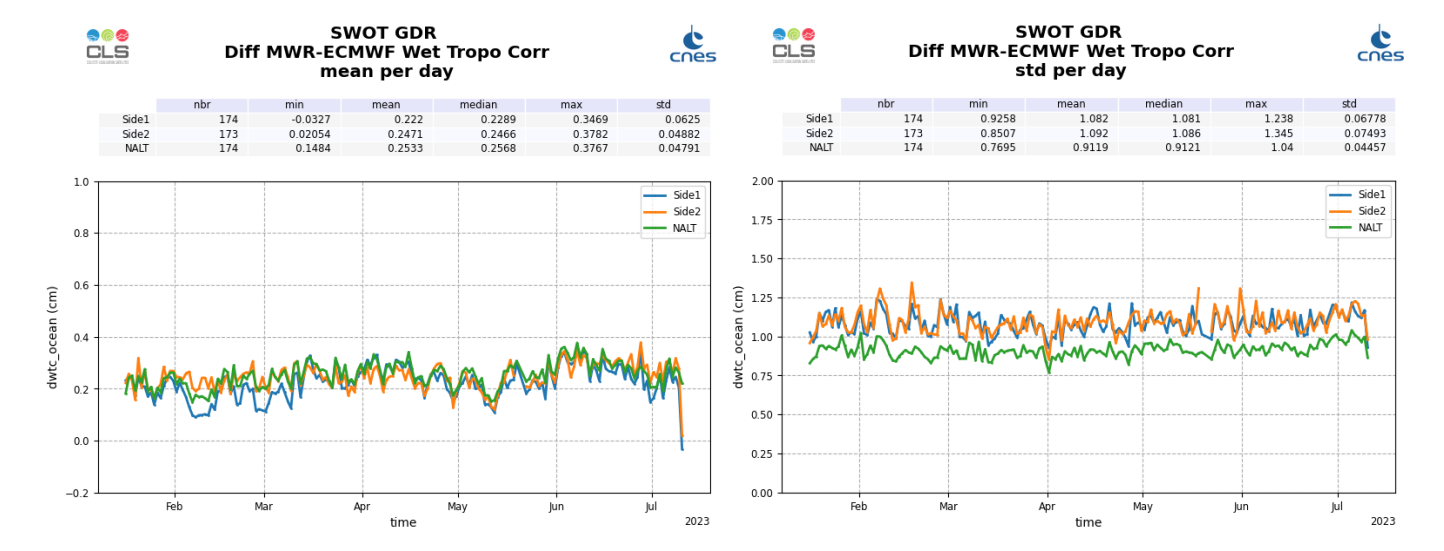


Figure 53: Daily monitoring of the mean of the Wet Tropospheric Correction for the AMR S1 (blue), AMR S2 (orange) and Nadir (green) for the entire calval phase

The other radiometer products (Water Vapor Content, Cloud Liquid Water Content, Atmospheric Attenuation for the Sigma 0) are interpolated the same way as WTC and can be compared to values issued from the ECMWF operational model too, as shown in figure 54, assessing the good temporal stability of the Atmospheric Attenuation, and the alignment between the measures from both radiometer sides and measures interpolated at Nadir.

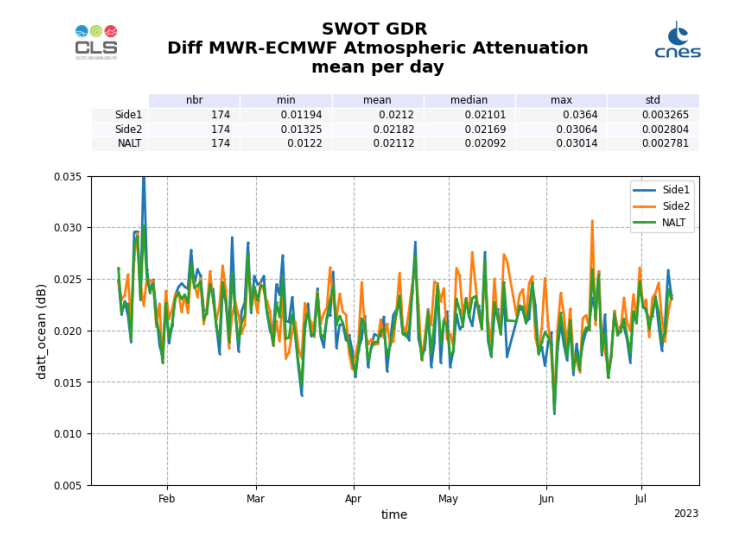


Figure 54: Daily monitoring of the mean of the Wet Tropospheric Correction for the AMR S1 (blue), AMR S2 (orange) and Nadir (green) for the entire calval phase

5.2 Comparison with Sentinel-6A

Figure 55a shows the daily mean difference between MWR-derived wet tropospheric correction and ECMWF-derived wet tropospheric correction for SWOT Nadir and Sentinel 6A-MF. There is a higher bias between the model and the MWR-derived correction for SWOT Nadir than for Sentinel-6A-MF (0.22 cm and 0.02 cm respectively), within the acceptable range, which results of a different choice for the calibration of the radiometer.

Figure 55b shows the daily standard deviation of the difference for SWOT Nadir, SWOT AMR S1, and



Sentinel-6A-MF. The standard deviation of the difference for Sentinel-6A-MF and SWOT AMR S1 are close (respectively 1.05 cm and 1.10 cm), indicating similar performances for the radiometers (Side 2 provides similar results than Side 1). The smaller standard deviation of the difference for SWOT Nadir (0.95 cm) is a direct consequence of the interpolation process which causes excessive smoothing to the data.

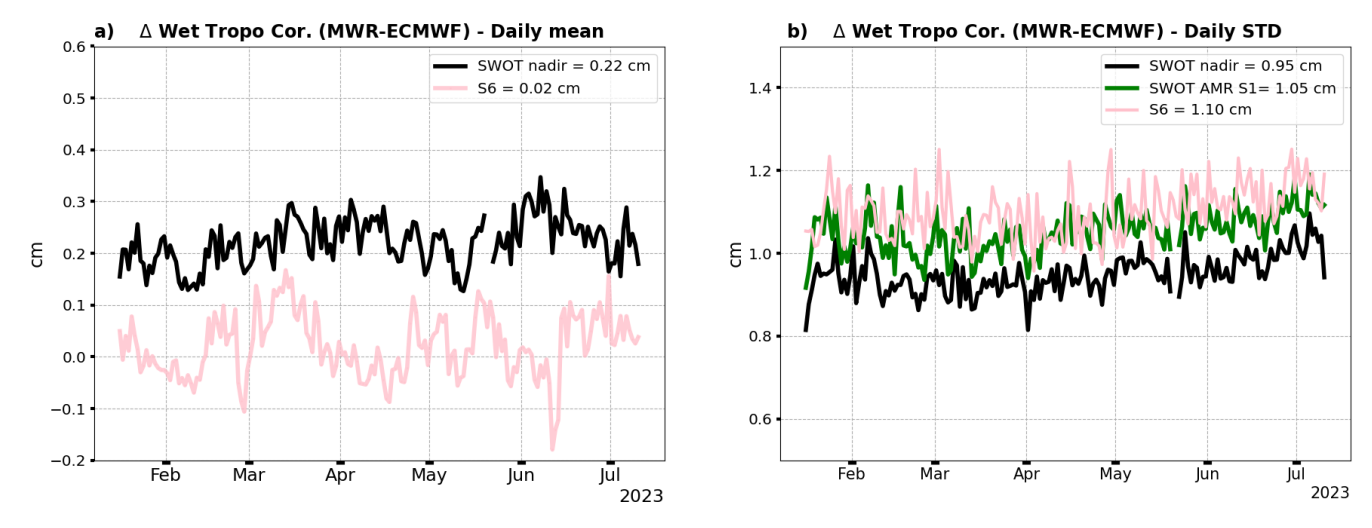


Figure 55: Comparison of MWR-derived wet tropospheric correction for SWOT Nadir (black solid line) and Sentinel-6A-MF (pink solid line) with those from ECMWF model. (a) Daily mean of Wet Tropospheric Corrections difference (b) Daily standard deviation of Wet Tropospheric Corrections difference, also for AMR Side 1 (green solid line).

5.3 Intercalibration monitoring

To assess the intercalibration between the two sides of the radiometer, the gradient between each Side 1 AMR measurements and the closer Side 2 AMR measurements is calculated for the three brightness temperatures and the Wet Tropospheric Correction. This monitoring allows to detect any instrumental drift affecting one of the radiometer beams, which whould increase the gradient between the two radiometer sides. In addition, excessive differences in measurements between the two beams would affect the quality of the interpolation at Nadir. Figure 56 shows the brightness temperatures gradients between the two radiometer beams. The gradient is small for the three channels (0.2 Kelvin for the 18.7 GHz and 23.4 GHz channels, and 0.3 for the 34 GHz channel), and with little fluctuations.



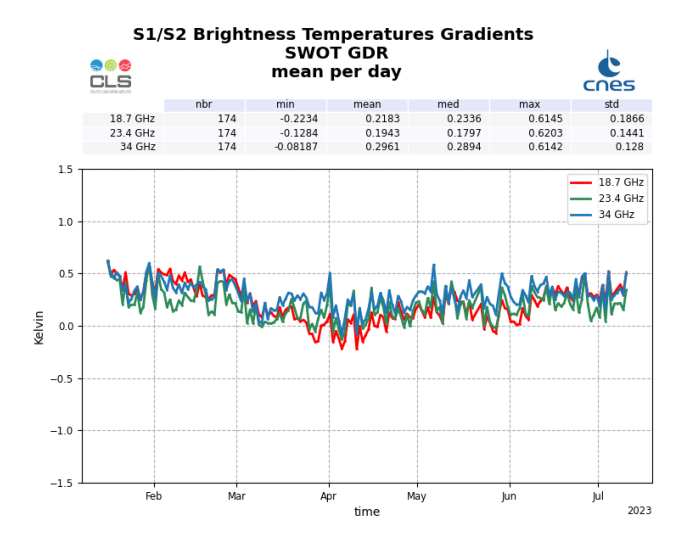


Figure 56: Daily monitoring of the mean S1/S2 gradients of brightness temperatures, for the 18.7 Ghz channel (blue), the 23.4 GHz channel (green) and the 34 GHz channel (red)

Figure 57 shows the Wet Tropospheric Correction gradient between the two radiometer beams and between the radiometer beams and the Nadir. This difference is stable and almost null for all the entire period, with difference between the two beams less than 1 mm, and with Nadir a little closer to S1, which is expected with the configuration of the radiometer beams.

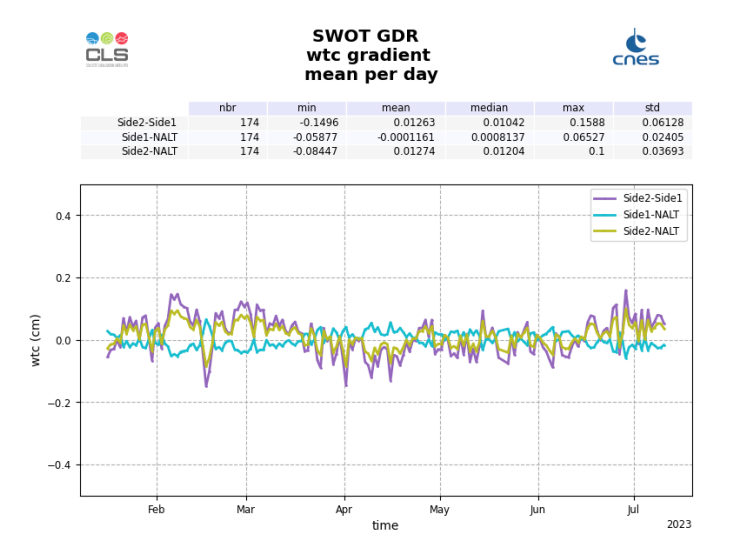


Figure 57: Daily monitoring of the wet tropospheric correction gradient between AMR Side 1 and AMR Side 2 (purple), AMR Side 1 and Nadir (cyan)

5.4 Degraded interpolation

For the GDR-S2 standard, the Nadir interpolation quality flag has 3 possibles values:

- 0: "Nominal" where the interpolation is succesfull computed using the two radiometer beams.
- 1: "Degraded" where the interpolation is computed with only one radiometer beam due to the invalidity of measurements from the other beams (due to rain cells, ice, or presence of land) or the interpolation is impossible and only the closest valid radiometer measurement is extrapolated to the Nadir point.
- 2: "No interpolation" where both the interpolation and the extrapolation mentioned in the previous case



are impossible and thus the radiometer value doesn't exist at the Nadir point.

Figure 58 shows an example where the interpolation is degraded and realized with only one radiometer beam, creating discontinuities in the Nadir wet tropospheric correction, which has an impact on the Sea Surface Heigh measurements quality.

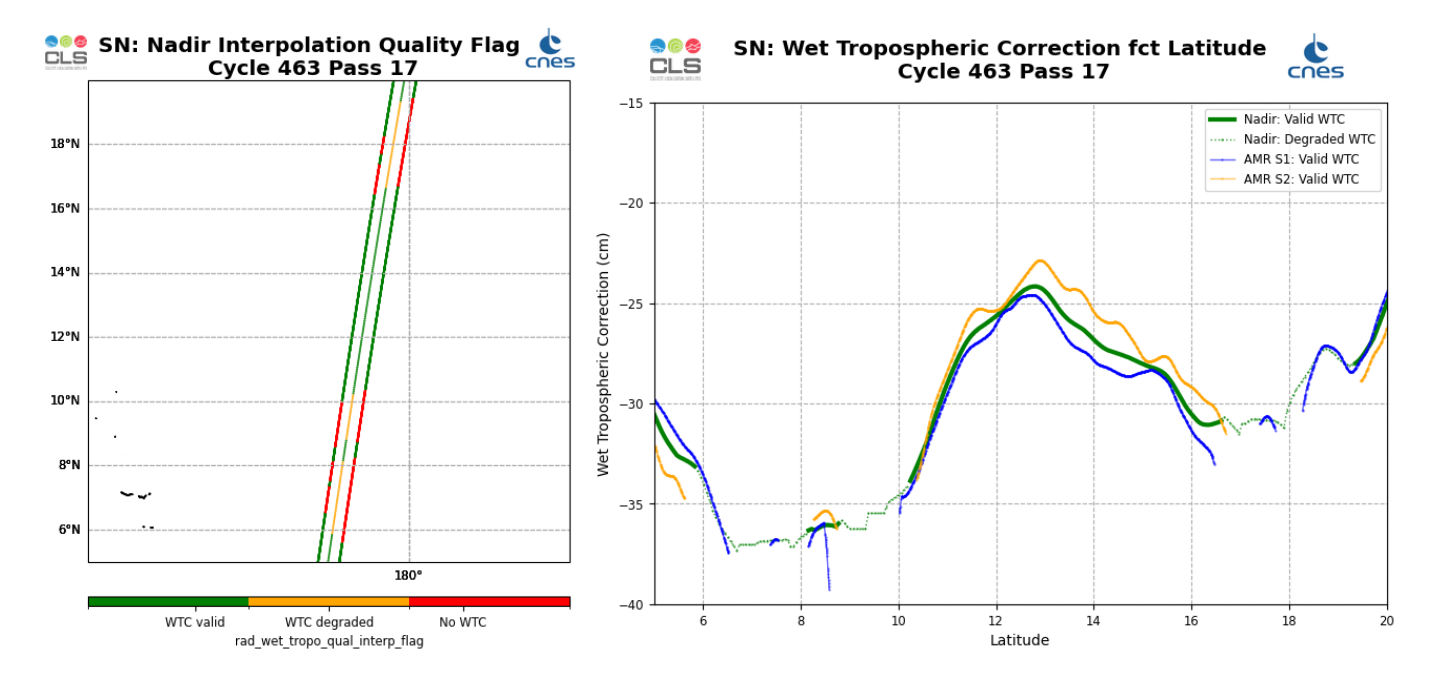


Figure 58: Left: Example of area where the Nadir interpolation quality flag is raised as degraded (orange) due to the rejection of radiometer measurements (red). Right: Evolution of the wet tropospheric correction depending on the latitude in the same example as the left figure, for both AMR sides (Blue and Orange, only valid measurements shown) and Nadir (plain green: valid WTC, dotted green: degraded wtc)

Figure 59 shows the percentage of poorly interpolated (i.e. with interpolation flag equal to 1 or 2) measurements by box of 1 degree of Lon/Lat. Most impacted areas are the ones strongly impacted by rain cells, in the intertropical convergence zone, and eastern pacific with up to 8% of points degraded or no interpolated.

Table 7 shows the global distribution of the Nadir interpolation flag values in open ocean (i.e. radiometer surface type flag indicates open ocean for both sides, and radiometer ice flag is not raised for both sides). This confirms the good coverage of radiometer products interpolated at Nadir with 98.4% of open ocean Nadir data correctly interpolated.

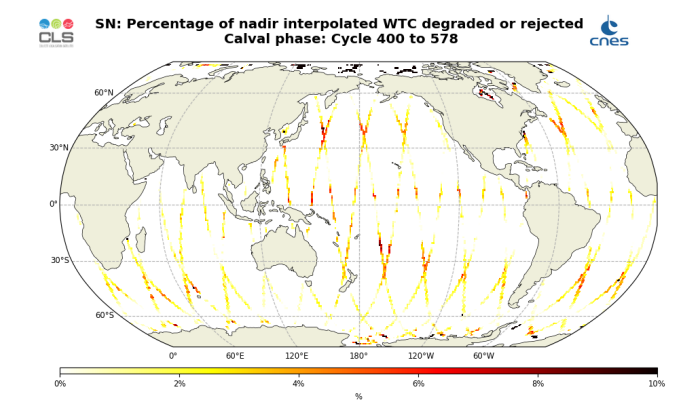


Figure 59: Proportion of degraded and missing Nadir interpolated wet tropospheric correction by geographical box of 1 degree



State of interpolation flag	percent
Valid	98.4 %
Degraded	1.44 %
No interpolation	0.16 %

Table 7: Proportion of each Nadir interpolation quality flag state in open ocean



6 Multimission comparison

6.1 Assessment from crossover analysis

Sea Surface Height crossover differences are the SSH differences between ascending and descending passes where they cross each other. Sea Surface Height is computed as follow:

$$SSH(corrected) = Orbit - AltimeterRange - \sum (GeophysicalCorrections)$$

with for SWOT Nadir:Orbit = CNES orbit for GDR products, and

 \sum (Geophysical Corrections) = Non parametric sea state bias correction

+ Dual frequency ionospheric correction (filtered)

+ Radiometer wet troposphere correction

 $+ \quad Dry \ troposphere \ correction$

+ Dynamical atmospheric correction

+ Ocean tide correction (including loading tide and non equilibrium tide)

 $+ Internal\ tide\ correction$

+ Earth tide height

+ Pole tide height

Sea Surface Height crossover differences are the SSH (corrected) differences between ascending and descending passes where they cross each other. Crossover differences are systematically analysed to estimate data quality. SSH crossover differences are computed from the valid data, with a maximum time lag of 10 days, in order to limit the effects of ocean variability which are a source of error in the performance estimation. The mean SSH crossover differences should ideally be close to zero and standard deviation should ideally be small.

Nevertheless, SSH varies also within 10 days, especially in high variability areas. Furthermore, due to lower data availability (due to seasonal sea ice coverage), models of several geophysical corrections are less precise in high latitude. Therefore, an additional geographical selection - removing shallow waters, areas of high ocean variability and high latitudes (> |50| deg) - is applied on temporal plots only and referred as "SL2".

Dual-mission crossover performances are computed between SWOT Nadir GDR-S2 and Sentinel-6A-MF GDR-F and presented in figures 60 and 61. Figure 60 displays the particular spatial distribution of crossovers points as well as the temporal distribution impacted by the 4 major coverage events listed in table 5. Figure 61 displays the monitoring of the mean and standard deviation of SSH difference at crossovers (top) and the maps of the mean of SSH difference at crossovers (4 by 4 degrees by bins) (bottom). At crossover points, on valid SL2 points, bias between the two missions is -3.18 cm and standard deviation is stable around 5.41 cm. These results highlight the consistency between the two missions. A more detailled comparison analysis based on daily DUACS grids is made in the Section 6.2.



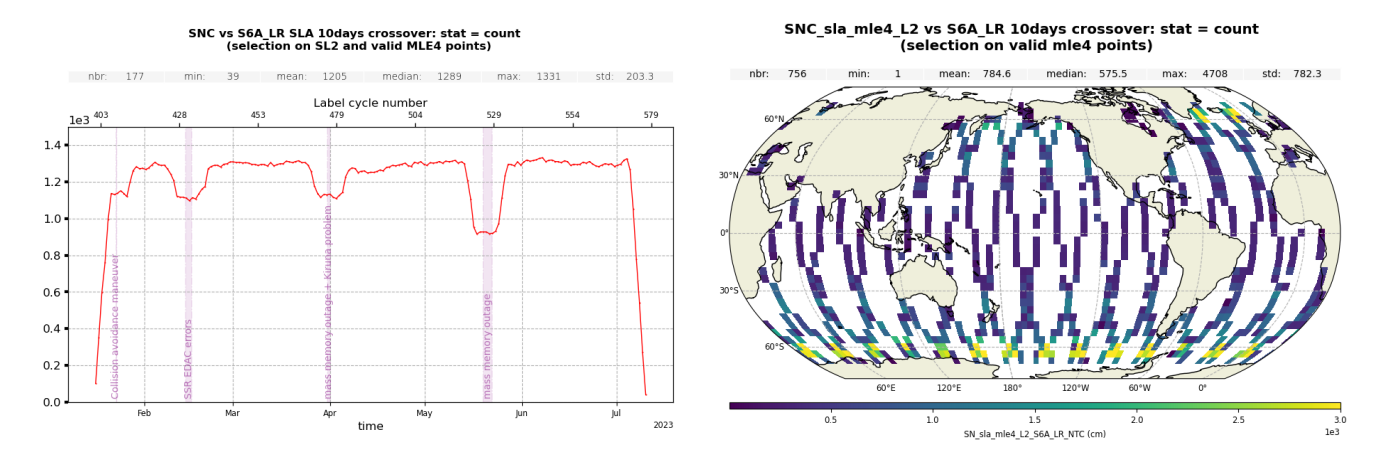


Figure 60: Count daily monitoring of SSH difference at crossovers between SWOT Nadir and Sentinel-6 MF LR

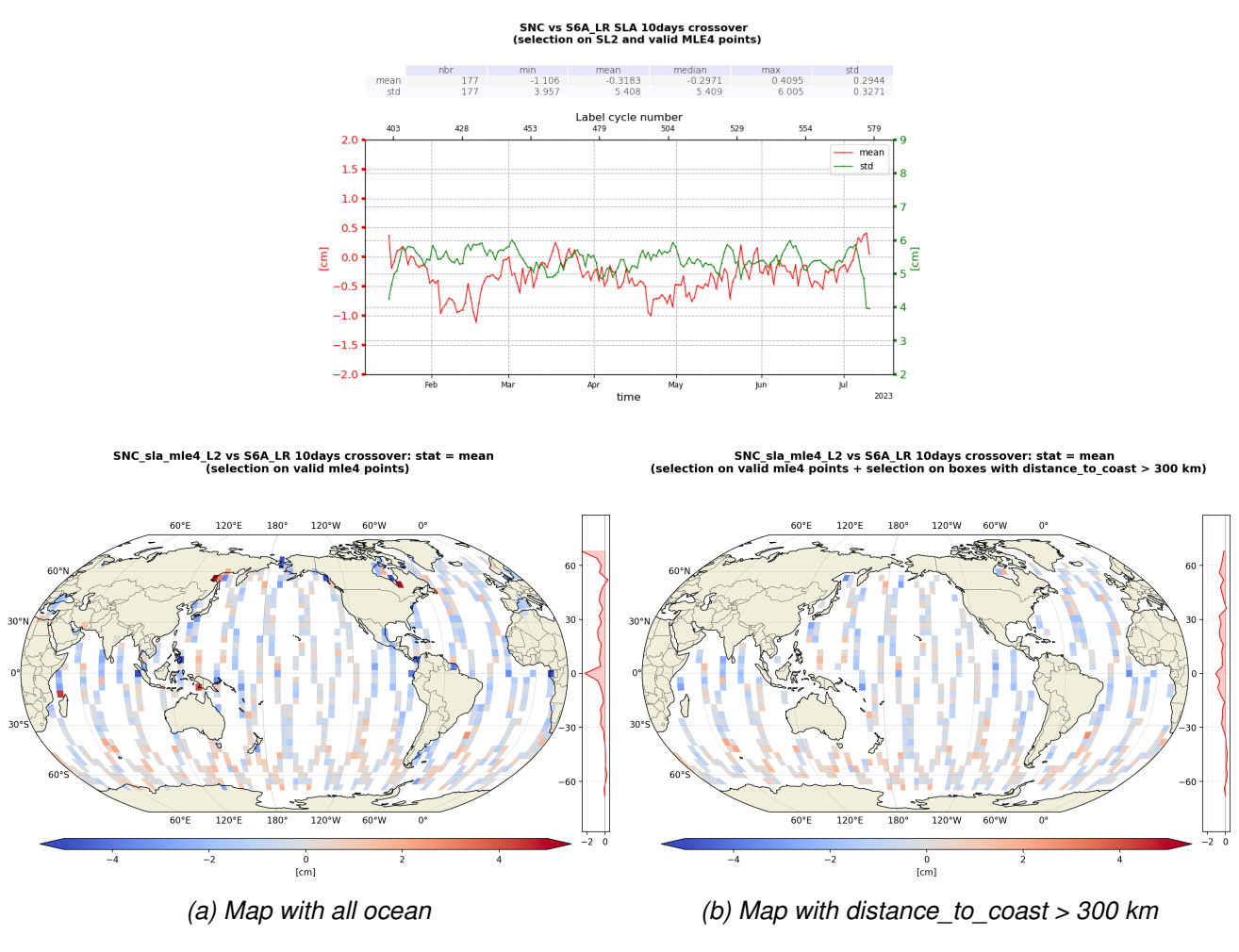


Figure 61: SSH difference at crossovers between SWOT Nadir and Sentinel-6 MF LR



6.2 Comparison to DUACS DT-24

SWOT Nadir SLA is compared to DUACS (Data Unification and Altimeter Combination System) DT-24 grids. It is a gridded multi-mission and inter-calibrated product that provides global grids of SLA daily. The description of the product is available here [12].

Gridded DUACS SLA is interpolated over the Nadir track using bilinear interpolation. The comparison is performed over valid points that correspond to ocean (surface_classification_flag=0). To suppress any ambiguity the difference clip that we study in the following figures is: DUACS_SLA - SWOT_Nadir_SLA.

The following figures show global and regional bias between DUACS and SWOT Nadir which comes from the altimeter inter-calibration processing of DUACS over the reference missions (from the first one TOPEX until S6A today).

In Figure 62, the daily mean global bias is 3.85 cm with a low associated standard deviation of 0.252 cm.

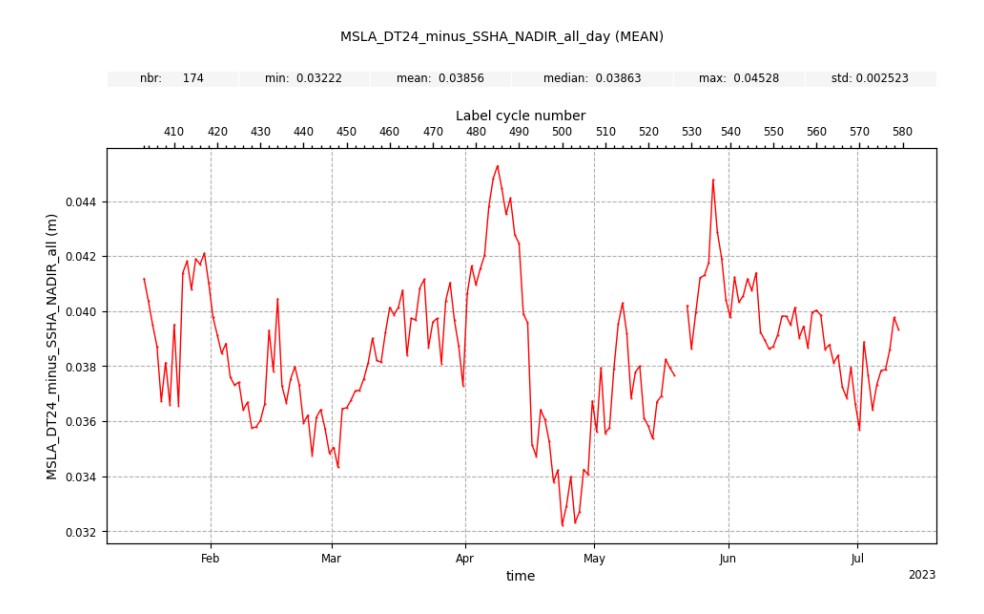


Figure 62: Daily monitoring of the mean bias between DUACS and SWOT Nadir SLA

We analysed the latitudinal dependency of the bias between DUACS and SWOT Nadir with a 2-dimensional time/latitude plot in Figure 63 and monthly global maps with both arcs, with ascending arcs only and with descending arcs in Figure 64.

The amplitude of this bias varies significantly over time. For example, in May, it can reach 3 cm (\pm 1.5 cm for latitudes < \pm 40° and \pm 1.5 cm for |latitudes| < 20°). However, the latitudinal dependency of the bias can be less important like it is the case in June.

In the monthly maps (Figure 64), geographical coherent biases are clearly visible and vary with time ($\sigma \in [1.1cm, 1.4cm]$). The explanation of these geographical biases have not been explained yet but an investigation which study the impact of the Precise Orbit Determination (POD) solution is ongoing.



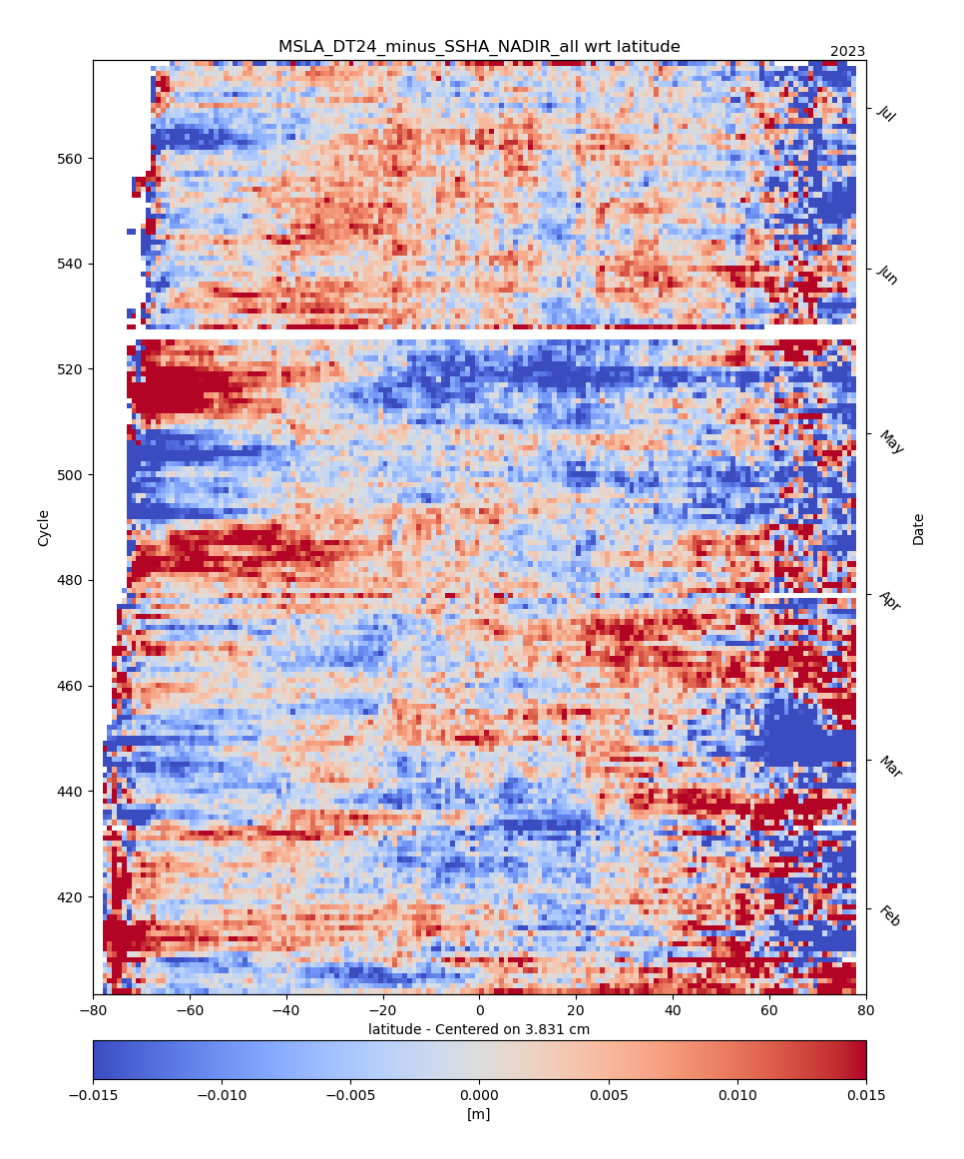


Figure 63: Daily monitoring of the latitudinal mean bias between DUACS and SWOT Nadir SLA



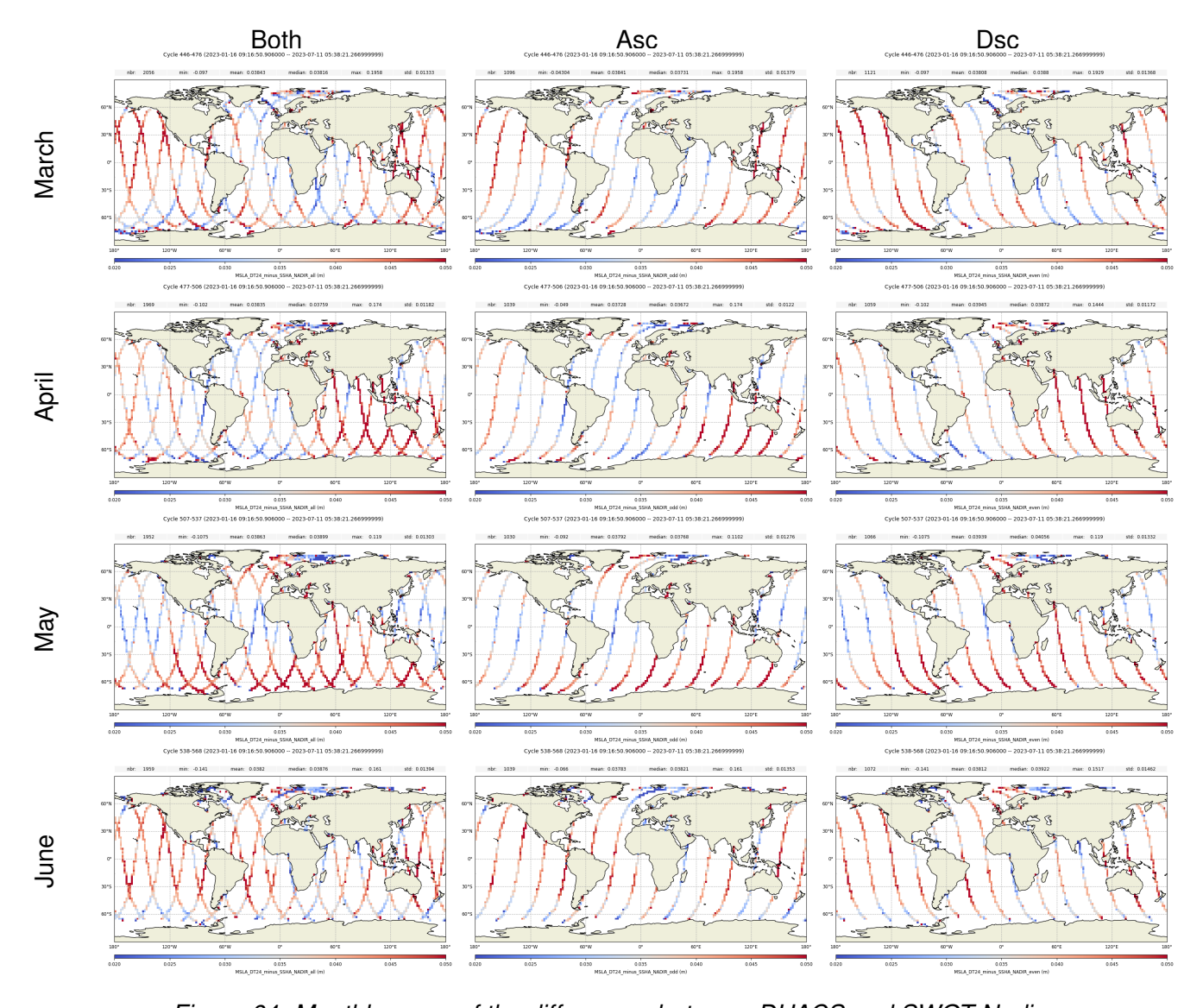


Figure 64: Monthly maps of the differences between DUACS and SWOT Nadir

6.3 Mean and Standard deviation of SSHA

The Sea Surface Height Anomaly (or sea level anomaly (SLA)) is the most well-known parameter estimated from altimetry. It corresponds to the elevation of sea surface, with respect to a reference called Mean Sea Surface (Mean Sea Surface (MSS)), generated by oceanic variability and climatic phenomena (such as Gulf stream current, El Nino, ...).

It is computed as follow:

$$SLA = Orbit - AltimeterRange - \sum (Geophysical Corrections) - MSS$$

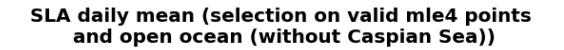
The details of the geophysical corrrections for SWOT Nadir can be found in previous section 6.1.

SLA analysis is a complementary indicator to estimate the altimetry system performances. It allows to study the evolution of SLA mean (detection of jump, abnormal trend or geographical correlated biases), and also the evolution of the Sea Level Anomaly (SLA) variance highlighting the long-term stability of the altimetry system performances.

It is important to note that J3 and S6A are on the orbit of reference covering most of the ocean. On the contrary during the 1-day calval phase SWOT covers a limited part which does not represent entirely the ocean observed by J3 and S6A. Sea surface height anomaly is a metric very dependant to the MSS reference solution which is used to compute SSHA.



The daily monitoring of mean SLA for SWOT Nadir is computed in Figure 65 and for standard deviation in Figure 66.



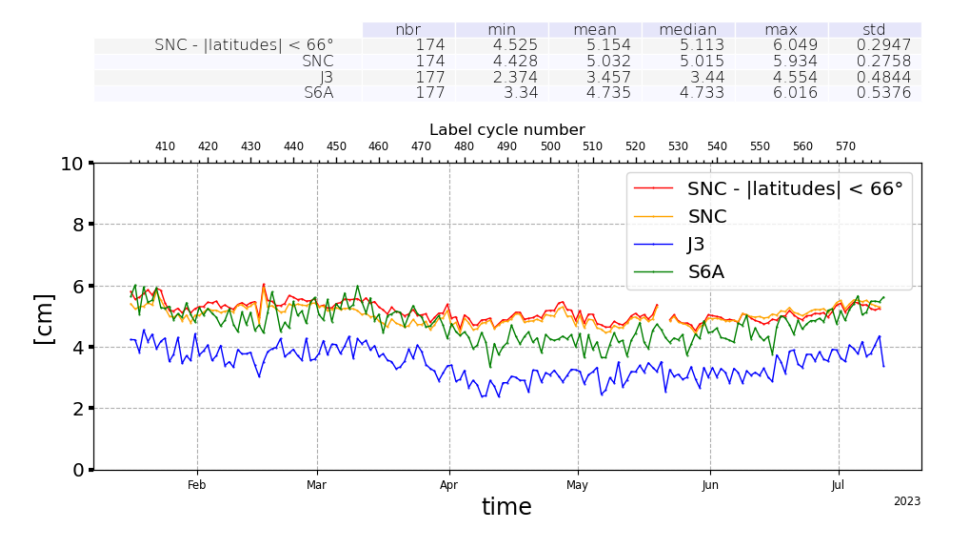


Figure 65: Daily monitoring of along-track mean SLA

SLA daily std (selection on valid mle4 points and open ocean (without Caspian Sea))

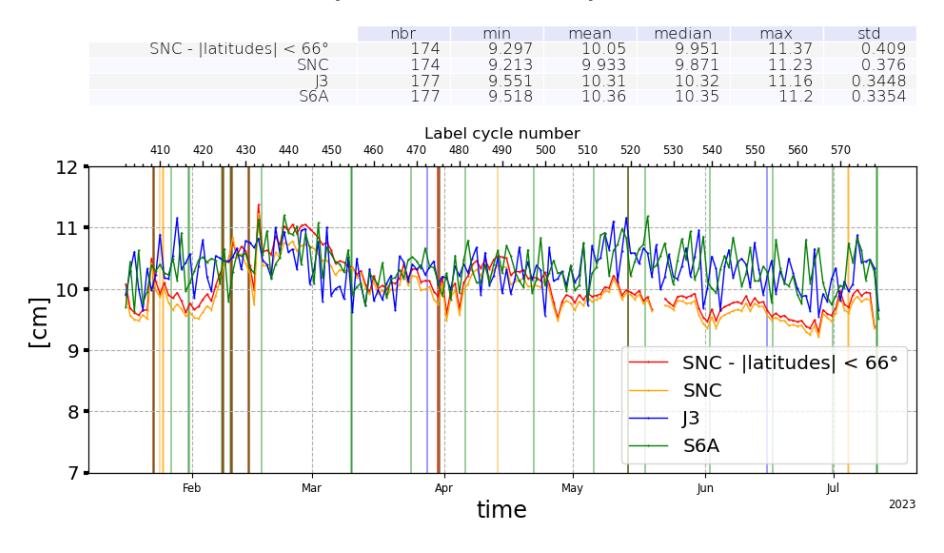


Figure 66: Daily monitoring of along-track std SLA

SWOT Nadir represents a coherent standard deviation level with regard to Jason-3 and Sentinel-6A until the end of April 2023 when SWOT Nadir level tends to be slightly inferior to the missions of reference. No explanation has been found yet.



7 Conclusions

SWOT Nadir was launched on December 16th, 2022. Until July 10th, 2023, SWOT Nadir was on its 1-day "calval" repetitive orbit phase.

The main points of the performance assessment are summarized below:

- Ocean data availability is great with a percentage of 94.8%.
- Data quality is also very good with 2.86% of rejected measurements over ocean (after removing sea ice data).
- The altimeter parameters analysis highlights a quite stable behaviour over the period.
- At crossovers, SWOT Nadir shows quite good performances with a standard deviation of 5.41cm and a good consistency with the Sentinel-6A-MF reference mission.

There are few known issues for SWOT Nadir:

- The current interpolation of radiometer data on the nadir track currently requires the two AMR sides to be defined and valid. When one AMR side is invalid (quality_flag_rad_wet_tropo_cor_qual), the nadir WTC can be affected by interpolation artifacts. Users who want to remove this subset of measurements can check the validity of the radiometer data and flags in the Radiometer L2 product (L2 RAD). In the next release, the SWOT Nadir processing will be updated to natively handle this border case: the radiometer flag (rad_wet_tropo_cor_interp_qual) in the L2 NALT will inform end-users of this degraded radiometer interpolation. In a future release, we plan to revisit the radiometer interpolation algorithm to mitigate or remove interpolation artifacts altogether.
- The adaptive retracker and Sea State Bias tables have not yet been calibrated for SWOT Nadir but on Jason-3 data.
- Some ionospheric correction measurements are lost due to a bad behaviour of the filtering process in rare cases. An ongoing study aims to explain this unexpected phenomenon.



8 Annexes

Cycle	Missing pass numbers	Comment
402	1, 2, 3	
404	11, 15	
407	26, 27, 28	
408	1, 2, 3, 4, 5, 6, 7, 8, 9, 10, 11, 25, 26, 27, 28	Collision avoidance maneuver
409	1, 2	
431	7, 8, 9, 10, 11	
432	15, 16, 17, 18, 19, 20, 21, 22, 23, 24, 25, 26, 27, 28	Data gaps due to SSR EDAC errors
433	1, 2, 3, 4, 5, 6, 7, 8, 9, 10, 11, 12, 13	
438	7	
476	26, 27, 28, 5	Many gaps on sevral passes due to high winds at Kiruna + mass memory outage
477	1, 2, 3, 4, 5, 6, 7, 8, 9, 10, 11, 12, 13, 14, 15, 16, 17, 18, 19, 20, 21	
504	6	
506	24, 25	
513	15	
525	26, 27, 28	
526	1, 2, 3, 4, 5, 6, 7, 8, 9, 10, 11, 12, 13, 14, 15, 16, 17, 18, 19, 20, 21, 22, 23, 24, 25, 26, 27, 28	Mass memory outage
527	1, 2, 3, 4, 5, 6, 7, 8, 9, 10, 11, 12, 13, 14, 15, 16, 17, 18, 19, 20, 21, 22, 23, 24, 25, 26, 27, 28	
528	1, 2, 3, 4, 5, 6, 7, 8, 9, 10, 11, 12, 13, 14, 15, 16, 17, 18, 19, 20, 21, 22, 23, 24, 25	
534	15	
566	2, 3	
578	4, 5, 6, 7, 8, 9, 10, 11, 12, 13, 14, 15, 16, 17, 18, 19, 20, 21, 22, 23, 24, 25, 26, 27, 28	End of fast orbit phase at pass 003

Table 8: Entirely missing passes



9 References

References

- [1] SWOT Nadir cyclic validation reports available at https://www.aviso.altimetry.fr/en/data/calval/systematic-calval/validation-reports/swot-nadir.html
- [2] SWOT mission description available at https://www.aviso.altimetry.fr/en/missions/current-missions/swot. html
- [3] SWOT Nadir Altimeter User Products guide available at https://www.aviso.altimetry.fr/fileadmin/documents/data/tools/SALP-ST-M-EA-17043-CN_0104.pdf
- [4] Jason-3 product handbook available at https://www.aviso.altimetry.fr/fileadmin/documents/data/tools/hdbk j3.pdf
- [5] SWOT Nadir GDR-S2 release note available at https://www.aviso.altimetry.fr/fileadmin/documents/data/tools/SWOT_L2_GDR_NALT_VersionS_Release_Note_20250516.pdf.
- [6] SWOT Nadir annual reports of validation activities available at https://www.aviso.altimetry.fr/en/data/calval/systematic-calval/annual-reports/swot.html
- [7] Guérin A., Piras F., Cuvillon N., Homerin A., Le Gac S., Maraldi C., Bignalet-Cazalet F., Alves M., and Rey L. 2024. Description and In-Flight Assessment of the POSEIDON-3C Altimeter of the SWOT Mission. *Remote Sensing*, 16(22), 4183. https://www.mdpi.com/2072-4292/16/22/4183.
- [8] Brown G.S., "The average impulse response of a rough surface and its application", *IEEE Transactions on Antenna and Propagation*, Vol. AP 25, N1, pp. 67-74, Jan. 1977.
- [9] Thibaut, P. O.Z. Zanifé, J.P. Dumont, J. Dorandeu, N. Picot, and P. Vincent, 2002. Data editing: The MQE criterion. *Paper presented at the Jason-1 and TOPEX/Poseidon Science Working Team Meeting, New-Orleans (USA), 21-23 October.*
- [10] Nencioli Francesco, Roinard Hélène, Bignalet-Cazalet Francois. 2021. Filtering ionospheric correction from altimetry dual-frequencies solution. DOI 10.24400/527896/a02- 2021.001. Available at https://www.aviso.altimetry.fr/fileadmin/documents/data/tools/NT-Nencioli_FilteredIonosphericCorrection.pdf
- [11] Jason-3 validation of GDR-F data over ocean https://www.aviso.altimetry.fr/fileadmin/documents/calval/validation report/J3/SALP-RP-MA-EA-23480-CLS Jason3 Reprocessing Report v1-2.pdf
- [12] Global Ocean Gridded L 4 Sea Surface Heights And Derived Variables Reprocessed 1993 Ongoing description available at https://data.marine.copernicus.eu/product/SEALEVEL_GLO_PHY_L4_MY_008_047/description. DOI 10.48670/moi-00148.

